

ABSTRACT

Evaluating the Effects of Acute Diesel Exhaust Particle Exposure on P-glycoprotein Function and Expression in the Blood-Brain Barrier

Kaitlin Nunn

Director: Dr. Erica Bruce, Ph.D.

Diesel exhaust particles (DEP) are a major component of air pollution and a source of concern because once inhaled, DEP may reach the brain, contributing to neurodegenerative disorders. One of the blood-brain barrier's (BBB) main functions is to limit the entry/action of pathogens and xenobiotics like DEP. Specifically, P-glycoprotein (P-gp), a multidrug transporter found in endothelial cells of the BBB, is responsible for the efflux of small molecule drugs and harmful chemicals from the CNS. The goal of this study was to evaluate the effects of acute (24 hr.) DEP exposure on the function and expression of P-gp in the BBB, and in the BBB with microglia *in vitro*. We used RT-qPCR to measure P-gp expression, immunocytochemistry and fluorescent imaging to qualitatively analyze the presence of P-gp, and a Rhodamine-123 Accumulation Assay to measure the activity of P-gp in the endothelial cells. This work is significant because it is the first to evaluate the effect of DEP on P-gp of the BBB. The disruption of P-gp and the resulting dysfunction of the BBB may be implicated in air-pollution-related neurodegenerative disorders.

APPROVED BY DIRECTOR OF HONOR'S THESIS:

Dr. Erica Bruce, Department of Environmental Science

APPROVED BY THE HONORS PROGRAM:

Dr. Elizabeth Corey, Director

DATE: _____

EVALUATING THE EFFECTS OF ACUTE DIESEL EXHAUST PARTICLE
EXPOSURE ON P-GLYCOPROTEIN FUNCTION AND EXPRESSION IN THE
BLOOD-BRAIN BARRIER

A Thesis Submitted to the Faculty of
Baylor University
In Partial Fulfillment of the Requirements for the
Honors Program

By
Kaitlin Nunn

Waco, Texas

May 2022

TABLE OF CONTENTS

List of Figures.....	iv
List of Tables.....	v
Acknowledgments.....	vi
Chapter One: Introduction.....	1
Chapter Two: Specific Aims and Objectives.....	12
Objective I.....	12
Main Questions.....	12
Hypothesis.....	12
Plan of Action.....	13
Significance.....	16
Objective II.....	16
Main Questions.....	16
Hypothesis.....	17
Plan of Action.....	17
Significance.....	18
Chapter Three: Methods and Materials.....	19
Cell Culture.....	19
MTT Assay.....	22
Immunocytochemistry.....	23
Rhodamine-123 Accumulation Assay.....	25

Inhibitor Optimization.....	25
RNA Extraction, cDNA Conversion, RT-qPCR.....	27
Chapter Four: Results.....	30
MTT Assay.....	30
Immunocytochemistry.....	31
Rhodamine-123 Accumulation Assay.....	36
RNA Extraction, cDNA Conversion, RT-qPCR.....	38
Chapter Five: Discussion.....	40
Immunocytochemistry.....	40
Rhodamine-123 Accumulation Assay.....	41
RT-qPCR.....	42
Conclusion.....	43
Appendices.....	46
Appendix A: Cell Culture.....	47
Appendix B: MTT Procedure.....	50
Appendix C: Immunocytochemistry Procedure.....	51
Appendix D : Rhodamine-123 Accumulation Assay Procedure.....	53
Appendix E : RNA Extraction, cDNA Conversion, RT-qPCR Procedures.....	54
Bibliography/ References.....	60

LIST OF FIGURES

Figure 1: Schematic representation of diesel particulate matter (PM) formed during combustion of atomized fuel droplets. The resulting carbon cores agglomerate and adsorb species from the gas phase (taken from Twigg et al., 2009).....	1
Figure 2: DEP Routes of Entrance. Created by Kaitlin Nunn through BioRender	4
Figure 3: Schematic representation of the blood-brain barrier (BBB) and components of a neurovascular unit (NVU) (Taken from Abbott et al., 2006).....	7
Figure 4: Proper Fluorescence of ICC Antibody for ZO-1, Taken from Abcam.....	14
Figure 5: Proper Fluorescence of ICC Antibody for CD105(Green), Taken from Abcam.....	14
Figure 6: Proper Fluorescence of P-gp ICC, Taken from Abcam.....	15
Figure 7: Human Immortalized Endothelial Cell Culture (D3), Light Microscopy (5x), Bruce Lab	19
Figure 8: D3 cells with Human Immortalized Microglial Cells (hMC3s), Light Microscopy (5x), Bruce Lab.....	21
Figure 9: DEP Particles, Transmission Electron Microscope Image (25,000x), Bruce Lab.....	22
Figure 10: MTT Assay Principle, Taken from www.technologyinscience.com Video Lecture.....	22
Figure 11: Concentration-Response Curve of DEP in hCMEC/D3s (24 hr. exposure).....	30
Figure 12: ICC Slides for ZO-1 and CD105, Fluorescence Microscopy, Taken by Bruce Lab.....	31-32
Figure 13: ICC Slides for P-gp, Fluorescence Microscopy, Taken in Bruce Lab.....	33-35
Figure 14: Rhodamine-123 accumulation assay demonstrates Rhodamine-123 accumulation that is inversely related to P-glycoprotein activity.....	36
Figure 15: RT-qPCR Relative Gene Expression.....	38

LIST OF TABLES

Table 1. P-values of Mann-Whitney U Test for Rho-123 Accumulation Assay Comparing BBB Control to DEP-Exposed BBB.....	38
--	----

ACKNOWLEDGMENTS

I am very thankful for the tremendous amount of help I have received in my time as an undergraduate student at Baylor University and would like to take a second to acknowledge all who have contributed to my success.

First, I would like to thank Dr. Erica Bruce, who graciously accepted me into her lab and mentored me throughout my thesis process. Dr. Bruce is perhaps one of the busiest and most diligent women I have had the great opportunity of knowing. On top of being the Graduate Program Director, an accomplished researcher, mother, and associate professor at Baylor, she took time out of her schedule to sit with me and discuss the research for my thesis.

Next, I would like to thank Ph.D. Candidate, Grace Aquino, my graduate student mentor who has helped me through everything. I just wanted to take the opportunity to truly appreciate all she has done for me, from helping me understand the rules of the Bruce Lab to helping me write my thesis, Grace has been there through it all and I am so grateful that she took the time to be involved in my life.

In the same regard, I would like to extend my appreciation to all my fellow undergraduate researchers in Bruce Lab who helped with the research that contributed to my thesis. Thank you, Katy Thomas, Bennett Schackmuth, Nazeel Shariff, Rishi Patel, Manu (Manogna) Jarajapu, and Morgan Pluto. I could not have completed this thesis without your help.

Of course, I would also like to thank my parents who helped me maintain my head as I went about writing my thesis. Their continued support throughout my entire college experience has allowed me to prosper at Baylor and not completely combust due to stress. I am extremely grateful for everything you have done for me, love you to the moon and back.

I would also like to thank Dr. Abel and Dr. Dean for not only agreeing to be on my thesis committee but also for the invaluable mentoring I have received from both. You are both such amazing role models for women in science and I hope you will continue to mentor aspiring researchers and scientists just as you have inspired me.

Lastly, I would like to thank all the professors I have had the opportunity to learn from. Without you I would not have finished college with the great depth of knowledge I now have, and I am forever grateful for you all.

CHAPTER ONE

Introduction

Urban areas and areas lacking regulation of industrial air pollutants have higher concentrations of particulate matter (PM) in the air than areas with regulated air pollution or a lack of concentrated diesel exhaust. A high concentration of particulate matter in the air has been linked to increased mortality and morbidity world-wide (Adar et al., 2014). Particulate matter (Figure 1) is a complex combination of many aerosolized chemicals. A major component of urban air particulate matter is diesel exhaust particles (DEP), a combination of a carbon core and heavy hydrocarbons, ash, metallic abrasion particles, sulfates, silicates, and polycyclic aromatic hydrocarbons (PAHs).

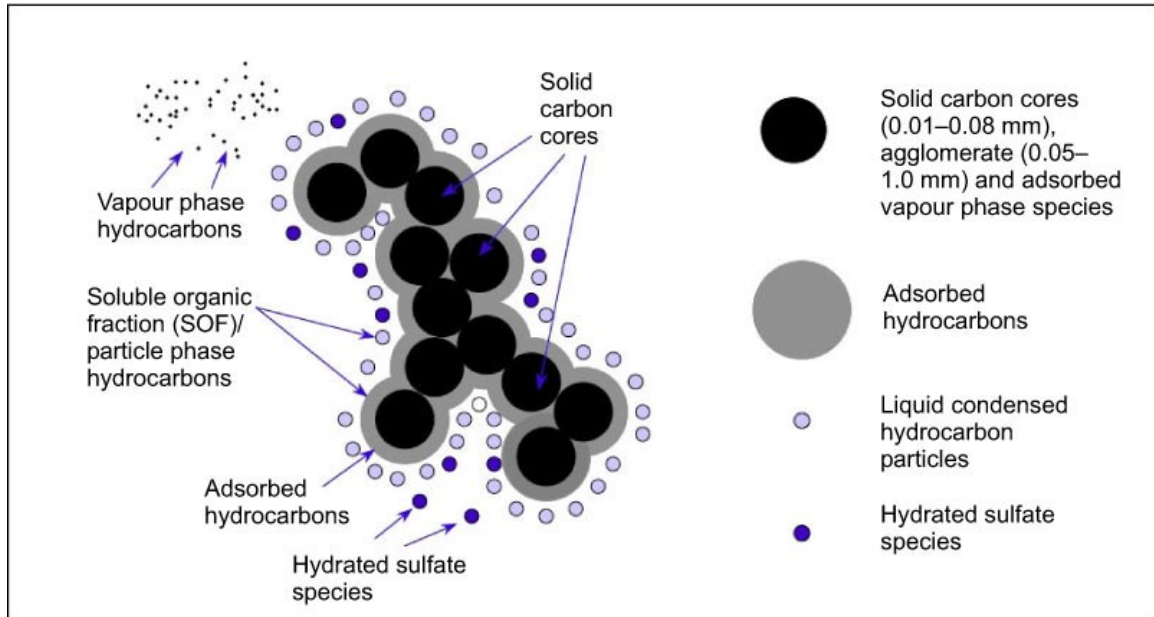


Figure 1: Schematic representation of diesel particulate matter (PM) formed during combustion of atomized fuel droplets. The resulting carbon cores agglomerate and adsorb species from the gas phase (taken from Twigg et al., 2009)

DEP are derived from the use of diesel fuels and lubricating oils (Wurzel, 2005). The United States Environmental Protection Agency (EPA) states that the size of the particulate matter found in the air is directly linked to their potential to cause harm in the human body (“What is Particulate Matter”, 2022). The most concerning are the particles that are 10 micrometers or less in diameter as these sizes would be inhalable and could pass through the throat and nose to enter the lungs or circulatory system. These are called “inhalable coarse particles” if their size ranges from 10 μm to 2.5 μm , “fine particles” if their size is less than 2.5 μm , or “ultra-fine particles” if their diameter is 0.1 μm or less (Kwon et al., 2020). Fine particles are of interest because they can remain suspended in the air for a longer time than larger particles and they are able to reach peripheral airways (Kwon et al., 2020). Ultra-fine particles are of significant concern because they cannot only reach peripheral airways, but they are also capable of entering the systemic circulation (Kwon et al., 2020). The size of DEP can range due to the fact that DEP are typically an agglomeration of multiple, primary particles that are about 15-40 nm in diameter (Burtscher, 2005). A study in 2005 found that aggregated DEP can be formed typically at a range of 60 nm to 400 nm, thus demonstrating DEP as having the possibility to present as both fine and ultra-fine particles (Burtscher, 2005).

Thus, although DEP exposure is very common, it is an environmental toxicant that can have significant negative health effects (Hartz et al., 2008). Acute exposure to DEP has shown to be an eye and nasal irritant, as well as cause changes in lung function and respiration, induce headaches, fatigue, and nausea (Sydbom et al., 2001). Chronic exposure to DEP is associated with an increased cough, sputum production, and lung dysfunction (Sydbom et al., 2001). The International Agency for Research on Cancer

(IARC), a sub-organization of the World Health Organization (WHO), classified Diesel engine exhaust as carcinogenic to humans in so much as that DEP exposure has a positive correlation to lung cancer (“Diesel Exhaust and Cancer Risk”, 2015). Of particular interest to this study are the effects of diesel exhaust particles (DEP) on human cells of the blood-brain barrier (BBB). DEP is known to cause oxidative stress and induce an inflammatory response in the brain (Cheng et al., 2016). The PAHs associated with diesel exhaust has been shown to induce the production of reactive oxygenation species (ROS) as well as decrease the activity of antioxidant enzymes in vascular endothelial cells (Wei et al., 2011). These components of DEP have also been shown to increase carcinogenesis (Pehncic & Jakovljević, 2018), cognitive decline (Best et al., 2016), and neuroinflammation in a mouse model (Hanghani et al., 2020). There has been increased interest in the involvement of DEP exposure in the development of central nervous system diseases, especially neurodegenerative diseases (Nel, 2005). Specifically, chronic exposures of the BBB to environmental chemicals like DEP has been implicated in the progression of diseases including vascular dementia, stroke, hypoxia, multiple sclerosis, Alzheimer’s disease (AD), Parkinson’s disease (PD), diabetes mellitus, and ischemia (Michalicova, 2020). Additionally, studies have found that BBB damage affects the accumulation of malformed proteins such as tau and amyloid- β , and that DEP exposure that correlates to BBB dysfunction is an extremely common pathophysiological identifier of Alzheimer’s Disease (Michalicova, 2020).

DEP currently have two known routes of impacting the human BBB and central nervous system (CNS), a direct pathway and a peripheral (indirect) pathway (Steiner et al., 2016).

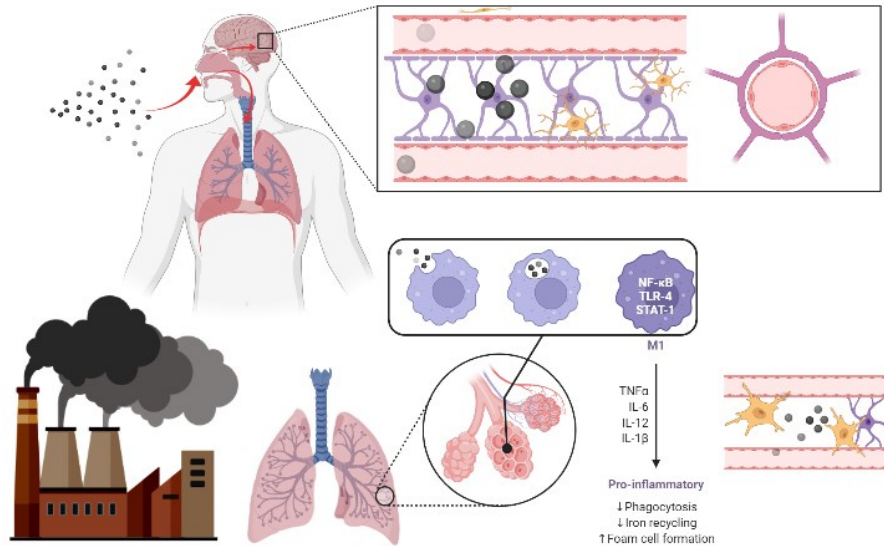


Figure 2: DEP Routes of Entrance. Created by Kaitlin Nunn through BioRender

The direct pathway is characterized by the inhalation or absorption of soluble DEP compounds through the olfactory bulb, directly into the CNS. It was discovered in rat models that more than 50% of ultra-fine particles can be deposited into the nasopharyngeal region upon inhalation (Oberdörster et al., 2008). Approximately 20% of the ultra-fine particles deposited onto the olfactory mucosa are capable of being translocated through the olfactory nerves to the olfactory bulb through diffusion, thus providing a possible mechanism for DEP to enter the brain while circumventing the blood-brain barrier (Oberdörster et al., 2008). Upon entrance, DEP can induce damage to the brain and spinal cord through the body's inflammatory response to xenobiotics such as DEP (Hartz et al., 2008). Thus, the DEP that has entered through the direct pathway

may also induce BBB dysfunction, microglial activation, oxidative stress, defective protein accumulation, astrogliosis, and even DNA damage (Cheng et al., 2016; Hartz et al., 2008; Oberdörster et al., 2008).

The peripheral (indirect) pathway is characterized by the absorption of DEP via an accessory organ such as the lungs. Once fine and ultra-fine DEP reach the alveoli, alveolar type II cells phagocytize the material and this can cause a time-dependent and dose-dependent stimulation of cytokines (Boland et al., 1999; Juvin et al., 2002). The cytokines produced by the alveolar type II cells can induce a pro-inflammatory response in the cardiovascular cells of the circulatory system as the cytokines are spread throughout the body which can eventually reach the BBB, inducing pro-inflammatory effects like damaging cellular junctions, proteins, membranes, lipids, and DNA (Nel, 2008). However, the BBB can be altered in different ways depending on the cytokines introduced, since some cytokines easily transverse the BBB, some must be engulfed via clathrin-independent lipid rafts to be brought across the BBB, while others are engulfed via clathrin-coated pits but are then degraded within the cell, and lastly some cytokines are not even allowed entrance into the endothelial cells (Pan et al., 2011). The effects of cytokines on P-gp expression and activity in rat brain capillaries has been measured in both a time- and dose-dependent fashion (Pan et al., 2011). The introduction of the cytokine TNF- α shows a biphasic effect, showing that lower doses decreased the expression and activity of P-gp, but longer exposure times (6 hours) showed an increase in the expression and activity of P-gp, which is most likely due to a difference in signaling pathway activation (Pan et al., 2011). It was also found that longer exposure times to TNF- α (72 hours) in human endothelial cells increased P-gp expression but

showed no change in transport activity (Pan et al., 2011). It was found that the introduction of cytokines which induce a continuous peripheral inflammation could be a major contributor to damage of the CNS, possibly connected to neurodegenerative disorders (Brook et al., 2004; Salter and Stevens, 2017; Süß, Lana, & Schlachetzki, 2021). However, there is no evidence that a single DEP exposure pathway is solely responsible for the development of CNS diseases, and it can be assumed that many pathways contribute to increased BBB and CNS dysfunction (Nel, 2008).

The BBB has been a major area of research because it is a selectively permeable membrane that tightly regulates the influx and efflux of substances between the vascular system and the CNS. This is a protective mechanism which effectively keeps toxins and harmful substances from the brain, however, it is also a hinderance in the realm of chemoresistance, often removing many pharmaceutical agents before they can reach their intended targets, the spinal cord or brain (Abu-Qare, 2003). The BBB functions within the wider context of the neurovascular unit (NVU), a dynamic system that works to maintain homeostasis and blood flow to the brain. The NVU is comprised of specialized cerebrovascular endothelial cells (ECs) which form the walls of blood vasculature in the CNS and are different from common peripheral tissue in that they often have fewer endocytic vesicles to limit the amount of transcellular flux (Rubin and Staddon, 1999). These specialized endothelial cells are coupled with tight junctions which severely limit paracellular fluctuation and forces molecules and other materials to enter the endothelial cell if the material wishes to enter the brain or spinal cord (Rubin and Staddon, 1999). However, the endothelial cells alone do not constitute the entirety of the NVU. Perivascular pericytes maintain BBB function. Astrocyte end-feet surround the

endothelial cells and contribute to the maintenance of the BBB and vessels dilation/constriction through chemical signaling (Kubotera et al., 2019). Neurons regulate the permeability of the BBB, and microglia, the most abundant CNS innate immune cell, closely associate with the BBB and CNS to protect from harmful agents (Alliot et al., 1999).

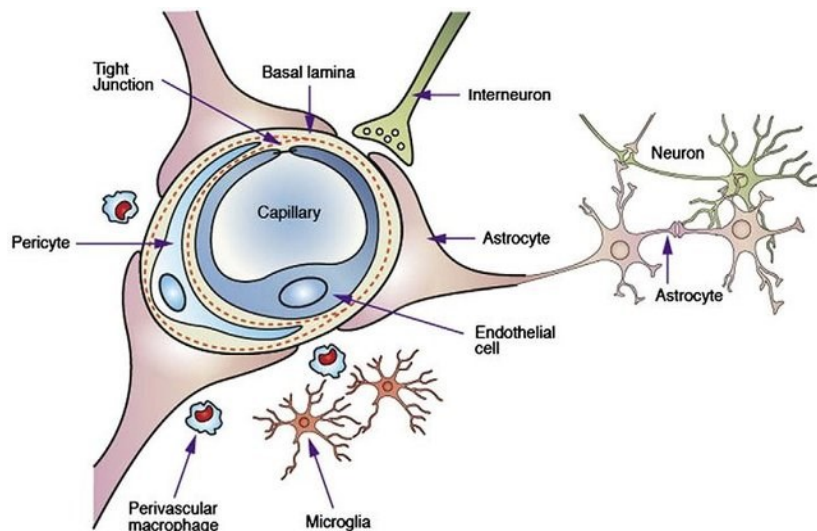


Figure 3: Schematic representation of the blood-brain barrier (BBB) and components of a neurovascular unit (NVU) (Taken from Abbott et al., 2006).

This study involved specialized transporter proteins on the cerebrovascular endothelial cells of the BBB. Of the many ATP-binding cassette (ABC) transporter proteins found in the BBB, one of the most prevalent and important is P-gp, a transmembrane protein capable of expelling a wide variety of xenobiotics, ions, metabolites, and possible therapeutics as they attempt to pass through the endothelial cells of the BBB (Miller et al., 2008). P-gp is abundantly produced on the luminal side of the cerebrovascular endothelial cells and plays a role in both neuroprotection and pharmacoresistance. Its ability to efflux molecules back into the lumen of the vascular system and limit the entry of foreign molecules to the brain is a protective function; however, it also contributes to the difficulty of drug delivery to the brain due to a limited

ability for medications to pass the BBB, which leads to pharmacoresistance (Qosa et al. 2015). P-gp has been considered the primary obstacle in the success of chemotherapeutics for brain tumors and contributes to the variability in patient responses to CNS medications (Löscher and Potschka, 2005).

P-gp, also known as ABCB-1 transporter protein, is an ABC transporter of the multidrug resistance (MDR) pump superfamily (Feltrin & Simões, 2019). It hydrolyzes ATP in order to efflux molecules from the interior of an endothelial cell to the exterior (Feltrin & Simões, 2019). For this to occur, the materials to be exported first are found inside the cell, with ultrafine particles this can occur via diffusion into the cell as well as vesiculation of toxic materials inside the cells. The cells then use efflux pump proteins to excrete this substance back into the lumen of the circulatory system. P-gp is a 170 kD protein comprised of two amino acid chains, each of which has six transmembrane domains and one nucleotide-binding domain, this allows for an extremely flexible protein that can alter its configuration for the efflux mechanism (Mollazadeh et al., 2018). Once a substrate enters a different binding domain, ATP bound at the nucleotide-binding domain will be hydrolyzed, this induces a conformational change in the transmembrane domains and catalyzes the efflux of the substrate through the transmembrane domain and lipid bilayer (Mollazadeh et al., 2018). ATP hydrolysis is also required for the proteins to return to their original conformation (Mollazadeh et al., 2018). The substrates transported by P-gp are variable; P-gp is known to transport cytotoxic drugs, xenobiotics, peptide antibiotics, steroid based hormones, immunosuppressive agents, calcium channel blockers and other molecules of varying size and function (Ueda et al., 1997). The only found commonality between a majority of P-gp substrates are aromatic rings, a basic

nitrogen in the substrate structure, hydrogen bond acceptors, and hydrophobic groups, all of which seem to play a role in binding affinity (Feltrin & Simões, 2019). However, these are not found in all molecules that modulate P-gp (Feltrin & Simões, 2019).

When exposed to DEP, studies have found that P-gp transcription and protein synthesis become upregulated within rat endothelial cells (Hartz et al., 2008). However, DEP exposure in an *in vitro* study was associated with decreased tight-junction protein expression and reduced the viability of the specialized cerebrovascular endothelial cells in rats (Wang, 2017). Moreover, the study found changes in the functionality and activity of P-gp, as well as the decreased expression of tight-junction proteins in rat cerebral capillaries after treatment with particulate matter due to circulating cytokines and reactive oxygen species (ROS) (Hartz et al., 2008). The introduction of DEP to the body causes an inflammatory reaction to occur wherein microglial cells excrete pro-inflammatory cytokines and ROS which increase oxidative stress in the BBB (Carson, 2002; Choi et al., 2016; Kreutzberg, 1996). This finding suggests that cerebrovascular endothelial cells could have an initial reaction to DEP that is different from long-term exposure (Choi et al., 2016). A study to determine P-gp's role in the BBB in Alzheimer's Disease (AD) found that when P-gp in the cerebrovascular endothelial cells is compromised, the cell is unable to properly export aberrant proteins (such as mutant Tau and amyloid- β) and thus provides some evidence that decreased P-gp function could be involved in the pathogenesis of AD (Wang et al., 2016). It has been found that an absence of P-gp, as in P-gp knock out mice, lead to an increase in the accumulation of amyloid-beta and caused an increased disturbance in the removal of amyloid-beta from the brain (Brucknamm et al., 2017). It has been shown in *in vitro* models of endothelial cells that P-gp can

transport amyloid-beta and that its dysfunction decreases amyloid-beta transport (Kuhnke et al., 2007; Lam et al., 2001).

Microglia are the innate immune cells of the CNS and play a critical role in the homeostasis of the brain environment by sensing invading microorganisms, searching for tissue damage, and clearing debris and foreign agents (Carson, 2002). Upon immunological stimulation, such as that following DEP exposure or an acute brain injury, microglial cells become activated (Kreutzberg, 1996). Due to the sensitivity of microglia, even small changes in their microenvironment can induce activation in response to injury or infection (Kreutzberg, 1996). Upon uptake of cytotoxic materials or cell-death indicators from outside the cells, microglial cells become “activated”, the activation is characterized by morphological changes of the microglial cells and secretion of soluble factors meant to induce change in surrounding cells (Lui & Hong, 2003). The majority of these secreted factors are considered proinflammatory and neurotoxic, including the cytokines tumor necrosis factor- α (TNF- α) and interleukin-1 (IL-1), as well as free radicals (nitric oxide and superoxide), and fatty acid metabolites (Lui & Hong, 2003). Studies have shown that in both in vitro and in vivo animal models excessive amounts of any individual proinflammatory factor excreted by the microglial cells can induce neurodegeneration (Boje and Arora, 1992; Chao et al., 1992; McGuire et al., 2001). However, the combination of factors has also been implicated in the degeneration of neuronal cells (Chao et al., 1995; Jeohn et al., 1998). Once activated, they release large amounts of tumor necrosis factor, TNF- α , which induces a pro-inflammatory response in the CNS that can cause damage to neuronal cells (Welser-Alves and Milner, 2013). The induction of TNF- α production by microglial cells has been shown to increase

paracellular permeability in the BBB endothelial cells, thus contributing to its dysfunction (da Fonseca et al., 2014). However, the effects of microglial activation on the expression of P-gp in the endothelial cells of the BBB are not well understood.

This study analyzed the effect of DEP on P-gp activity in human endothelial cells alone (i.e. monoculture), and in endothelial cells with microglial cells (i.e. co-culture). It is important to note that the co-culture of endothelial and microglial cells was not meant to simulate the NVU but rather it was formed as a 2D model to evaluate the effects of microglial cell interaction with endothelial cells in a non-directional model, analyzing P-gp expression and function. We hypothesized that, after acute exposure to DEP, the corresponding activity and expression of P-gp would increase in the endothelial cell monoculture in order to expel the DEP present within the media. We further hypothesized that DEP exposure to both endothelial and microglial cells in a co-culture, the activity of P-gp would increase, but to a lesser extent than in the monocultured cells due to cell layer dysfunction induced by proinflammatory cytokines.

CHAPTER TWO

Specific Aims and Objectives

The overall aim of this thesis was to evaluate the effect of acute diesel exhaust particle (DEP) exposure on P-gp found in endothelial cells of the BBB (i.e., monoculture of D3 endothelial cells) and in conjunction with hMC3 microglial cells (i.e. co-culture). This study evaluated the influence of microglia on the function and expression of P-gp in a 2D model of endothelial cells as a co-culture (microglial and endothelial cells combined) to determine if the microglial cells when acutely exposed to DEP influences the productivity of P-gp in the model.

Objective I

The first objective of this thesis was to evaluate the effect of acute (24-hour) DEP exposure on P-gp activity in human immortalized endothelial cells (D3).

The main question we addressed was:

1. How does acute exposure to DEP affect the expression and activity of the P-gp found in human immortalized endothelial cells alone?

Hypotheses:

1. Acute DEP exposure will cause an increase in expression and function of P-gp due to P-gp's role as an efflux pump in endothelial cells of the BBB.

Plan of Action:

In order to test these hypotheses, this study used different methods of analysis including a commercially available Rhodamine-123 Accumulation Activity assay that uses a fluorescent dye, Rhodamine-123 (Rho-123), to determine the activity of p-glycoprotein in the endothelial cells. We ran this assay to demonstrate the export of Rho-123 due to P-gp activity, increased activity would lead to a decreased concentration of Rho-123 inside the cell. If my hypothesis is correct, we expect to see a significant decrease of Rho-123 under exposure to the high concentration DEP, as the DEP should increase the activity of the P-gp in the endothelial cells, since P-gp is trying to expel the foreign substance.

Immunocytochemistry (ICC) is a technique used to demonstrate the presence of certain characteristics of cells by marking said characteristics with fluorescent antibodies. We used this method of research to characterize our endothelial cell line through the presence of ZO-1 and CD105, a BBB endothelial tight-junction protein and a human endothelial protein marker respectively.

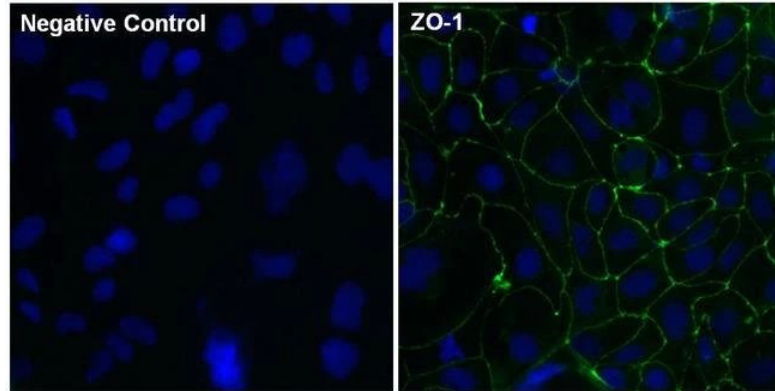


Figure 4: Proper Fluorescence of ICC Antibody for ZO-1, Taken from Abcam

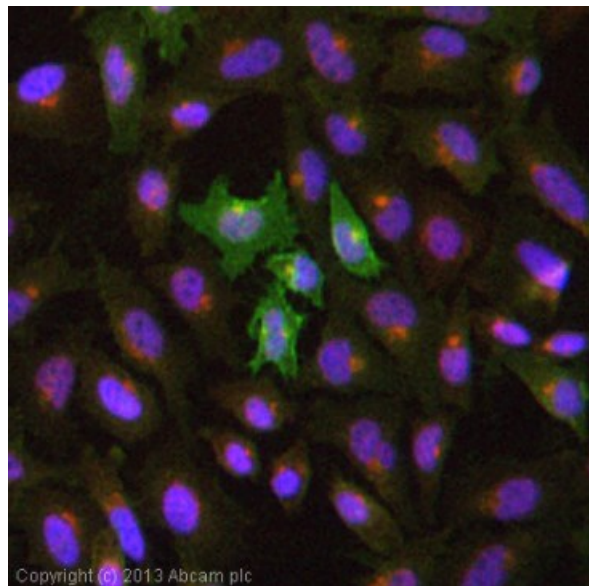


Figure 5: Proper Fluorescence of ICC Antibody for CD105(Green), Taken from Abcam

We used a P-gp monoclonal antibody to demonstrate the presence or change in production of P-gp in control versus DEP-exposed cells.

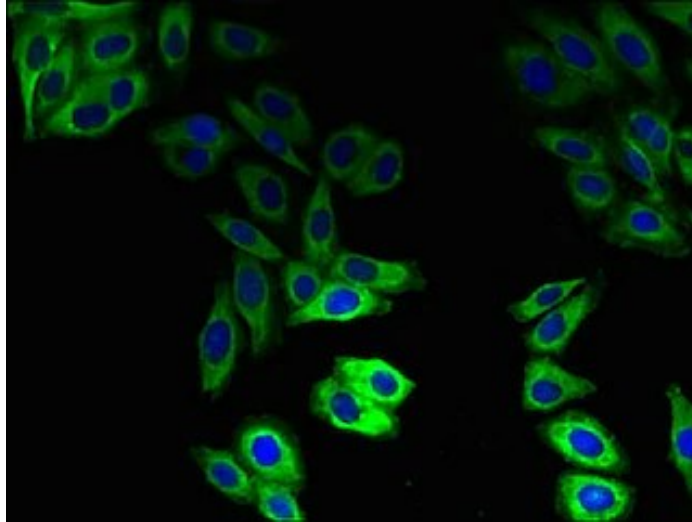


Figure 6: Proper Fluorescence of P-gp ICC, Taken from Abcam

DEP exposure could affect the formation and or the progression of neurodegenerative diseases, such as Alzheimer's, which is characterized by the dysfunction of P-gp in the endothelial cell of the BBB. If we were to demonstrate that DEP causes a significant increase in P-gp production, it could be noted that DEP exposure can possibly contribute to the formation of neurodegenerative diseases or cancers.

Utilizing quantitative reverse transcription PCR (RT-qPCR) we extract RNA that is first transcribed into complementary DNA (cDNA) by reverse transcriptase from total RNA or messenger RNA (mRNA) (“Basic Principles”). With this, we are able to see if there is an increased expression of P-gp mRNA and thus extrapolate that there would be an increased expression of P-gp’s efflux pumps on the cell’s surface. In this way, we are able to analyze both a control sample that is not exposed to DEP as well as a DEP treated group, testing the hypothesis that there is an increased expression of P-gp when acutely exposed to DEP.

Significance:

The significance of this experiment is that an analysis of the effects of acute exposure of DEP on P-gp of BBB human endothelial cells has not been previously investigated. The connection of P-gp activity to neurodegenerative diseases has been researched extensively. However, the inclusion of the specific analysis of the effects of DEP on the P-gp of endothelial cells of the BBB is yet to be studied and are the goals of this study to accomplish.

Objective II

The second objective of this paper is to analyze the effect of acute DEP-exposed human BBB endothelial cells and an acute DEP-exposed co-culture of human BBB endothelial cells and microglial cells to determine the effect of microglial activation on the P-gp activity in human BBB endothelial cells. This objective intends to explore the novel area of DEP exposure to an endothelial and microglial co-culture, specifically focusing on the P-gp activity associated with the activation of microglia and its effects on BBB function or dysfunction.

The main questions we address are:

1. How does acute DEP exposure in the human BBB endothelial cell and microglial cell co-culture effect P-gp expression and function?
2. How does acute DEP exposure to a human BBB co-culture change P-gp expression and function in comparison to a monoculture?

Hypotheses:

1. DEP exposure in the co-culture will cause an increase in P-gp expression but a decrease in P-gp function since the microglial cells secrete cytokines which could cause disruption the endothelial cells and could potentially limit P-gp pump efflux.
2. Acute exposure to DEP will induce a similar response in both the monoculture and co-culture.

Plan of Action:

First, we developed a co-culture consisting of the human immortalized endothelial cells (hCMEC/D3) in combination with human immortalized microglial cells (HMC3). This co-culture will then undergo analysis through the previously described P-gp assay, immunocytochemistry, and RT-qPCR methods of analysis.

We will continue to test the co-culture with the P-gp assay in order to determine if the presence of microglial cells in co-culture influence the P-gp activity of the endothelial cells. The co-culture will be assessed using the ICC methods mentioned in Objective I in order to qualitatively observe and analyze the presence of the marked structure, transporter proteins P-gp, in the both a control co-culture and a DEP-exposed co-culture.

Significance:

The significance of this study would be the novelty of examining the results of acute DEP exposure to a co-culture of human endothelial cells and human microglial cells. Specifically, analyzing the effects of DEP exposure on the activity of P-gp in the co-culture to understand the effects of microglial activation as a contributor to the dysfunction of the BBB when exposed to DEP. This can play a major role in the effect of

DEP on neurodegenerative disorder pathogenesis, since there are still gaps in the literature regarding the exact route of microglial effect on BBB endothelial cell dysfunction.

CHAPTER THREE

Methods and Materials

Cell Culture

The Blood-Brain Barrier hCMEC/D3 Cell Line (immortalized human endothelial cell line) was purchased from Sigma-Aldrich (product number: SCC066) (See Appendix A for complete care instructions). This cell line was chosen due to the literature, confirming its use in over 100 studies since 2005, as well as noting that the cells stain positively for multiple endothelial cell markers (CD34, CD31, CD40, CD105, CD144 (VE-cadherin), von Willebrand factor) except CD36, which is an endothelial cell marker not found in brain endothelium (Weksler et al., 2013). This cell line was also chosen due to its observance as an accurate model of the BBB (Weskler et al., 2013).

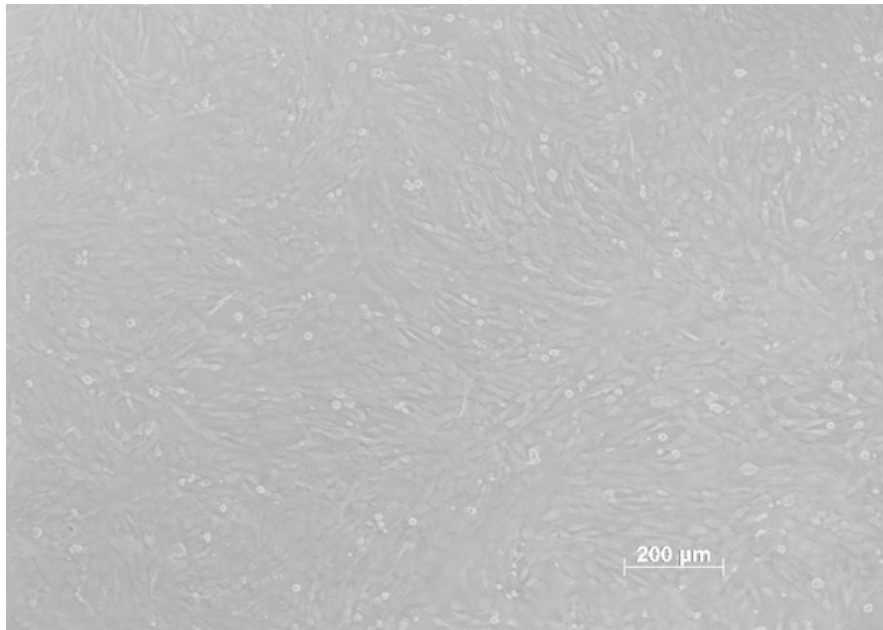


Figure 7: Human Immortalized Endothelial Cell Culture (D3), Light Microscopy (5x), Bruce Lab

The cells were cultured in an EndoGRO complete media from EMD Millipore (Product number: SCME004) The cells, which are stored in a vial kept in liquid nitrogen, were thawed using the recommended Millipore protocol for thawing of the hCMEC/D3 cell line. The cells were then maintained in a T-75 flask placed in a 37°C, 5% CO₂ humidified incubator. The cells were monitored daily for confluency and imaged to view overall growth and search for possible contamination. Once the cells reached 80% to 100% confluency then the cells were split into a new passage (Appendix A). During any splitting procedure the cell's density and viability was measured using the Countess II. The cells, now considered subcultures, were either frozen back for storage using 10% DMSO and slow-freeze (1 degree per min) containers, or they were added to new flasks/plates to form the next passage.

The immortalized human microglial cells, HMC3s, were purchased from ATCC (Product #: CRL-3304) and were maintained in an HMC3 media (See full care instructions in Appendix A). The cells received were either stored in liquid nitrogen or were placed in a T-75 flask for their cell line continuation in accordance with the company's recommended procedure. The flasks are kept in a 37°C, 5% CO₂ humidified incubator and are imaged daily. Once the cells reach a maximum of 3 million cells, they will need to be sub-cultured. The new cultures should be in accordance with guidelines, ensuring a concentration between 1×10^4 and 4×10^4 viable cells/cm², but not exceeding 7×10^4 cells/cm². Cells may also be frozen back using the same method as the D3 cells listed above. The co-culture consisting of both endothelial and microglial cells is intended to represent a 2Dimensional model of the interaction between the endothelial

cells and microglial cells in order to measure toxicity, P-gp activity, and P-gp genetic expression, not transport of DEP across a theoretical blood-brain barrier.

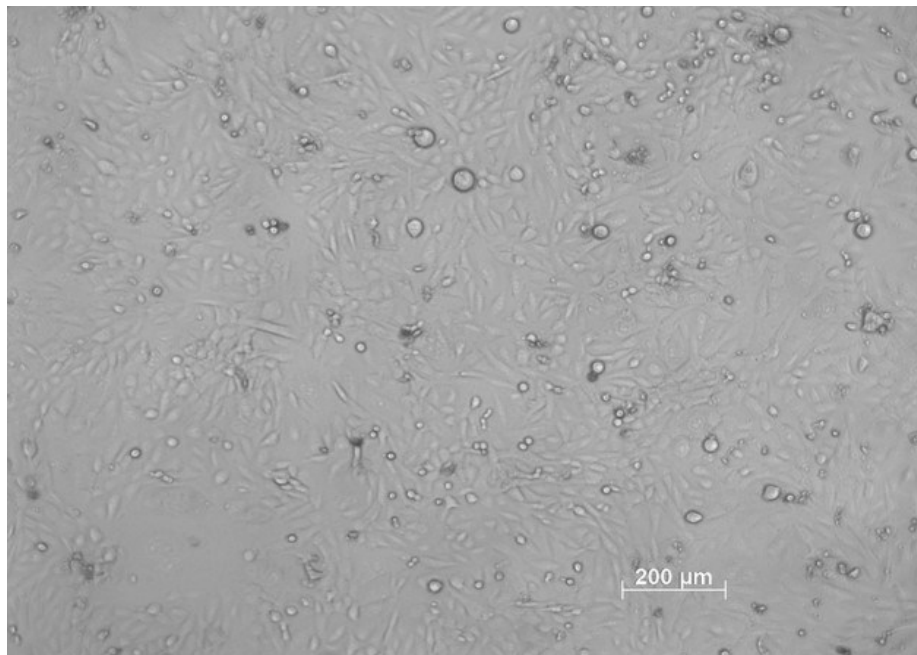


Figure 8: D3 cells with Human Immortalized Microglial cells (hMC3s), Light microscopy (5x), Bruce Lab

The DEP suspension was produced as a 2 mg/ml (2000 ug/ml) stock solution as prepared in Block et al.'s publication (Block et al., 2004). Briefly, 0.02 g of SRM2975 (NIST standard DEP) was added to 10 mL of PBS or water (or dosing media, no FBS) with 1% Dimethyl sulfoxide (DMSO) to allow for incorporation of the DEP into the media. This suspension was vortexed for 1 minute, then sonicated for 45 minutes utilizing an ultrasonicator, before it was warmed for 15 minutes in the 37°C-water bath. Before this media was used, it was sequentially filtered using various filter sizes down to 0.45 μm filter, to obtain fine DEP which contains ultra-fine DEP. This decision was made due to the standard NIST DEP size being 2.5 μm, and filtration beyond this size produced very small concentrations of DEP within the media. This media containing fine and ultra-

fine particles is then ready for use and can be used immediately or kept in the 4°C for up to 2 weeks. Here is shown a Transmission Electron Microscope (TEM) Image of the DEP in solution used throughout the study, this is at 25,000x magnification.

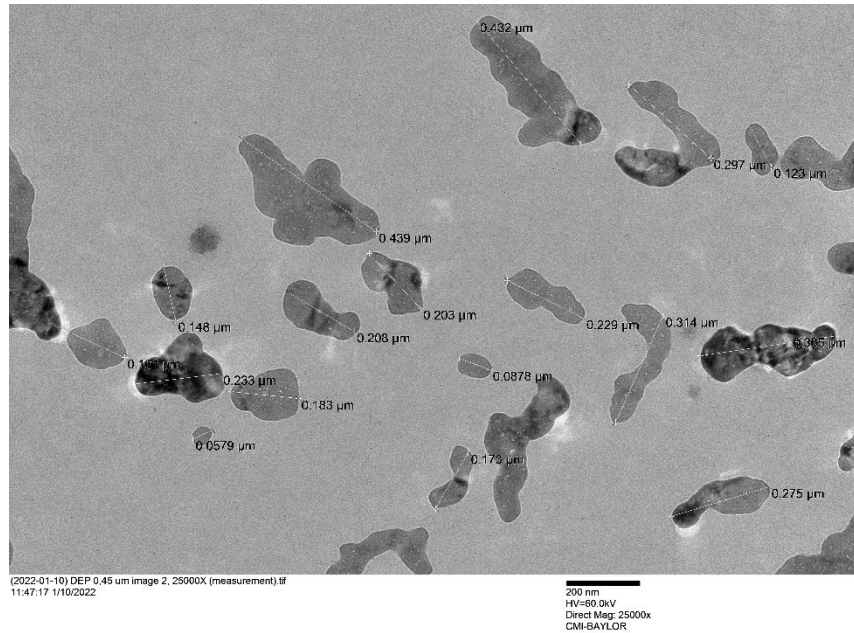


Figure 9: DEP Particles, Transmission Electron Microscope Image (25,000x), Bruce Lab

MTT

The MTT [3-(4,5-dimethylthiazol-2-yl)-2,5-diphenyltetrazolium bromide] assay is a colorimetric assay indicating cellular metabolic activity and cell viability. It is based on

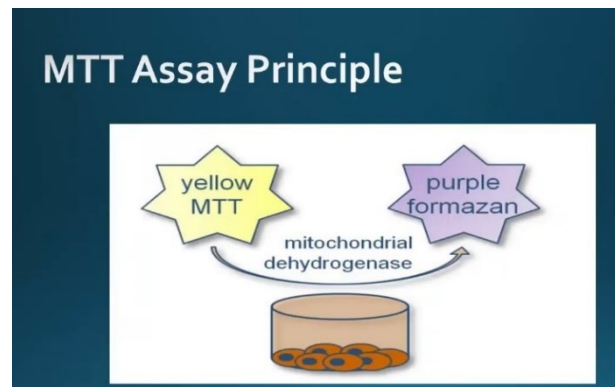


Figure 10: MTT Assay Principle, Taken from www.technologyinscience.blogspot.com Video Lecture

the action of intracellular NAD(P)H-dependent cellular oxidoreductase enzymes which reduces the MTT tetrazolium dye to an insoluble formazan product that is bright purple. The purple color is measured using a spectrophotometer at 595 nm, with 650 nm as a reference wavelength, and the absorbance is proportional to the number of viable cells. We plotted absorbance against concentration to determine the IC₅₀ and IC₁₀ of DEP, using both D3 (endothelial cells) and the HMC3 (microglial cells). The absorbance in each well was then measured at the 595-650 nm wavelength. (See full Procedure in Appendix B).

Immunocytochemistry

Immunocytochemistry is the process of attaching fluorescent antibodies to cellular components or proteins in order to view changes in a cell's morphology. This can be an especially useful tool in the lab to ensure cultured cells that have not transformed and indicate qualitatively if cell morphology has changed due to exposure to compounds or reagents. Before the process of immunocytochemistry began, the cells were grown on glass slides. Glass slides are preferred for this process due to the ease of imaging through the glass as compared to plastic since plastic can cloud images that need to be crisp and clear. These glass slides however are not optimal for cell growth without the use of coatings to allow cells to attach and form a cellular matrix (See Appendix C for full procedure).

The cells were then maintained in the 37°C, 5% CO₂ humidified incubator. Briefly, 24 hours after cells were seeded on glass slides, we exposed the cells to DEP (2000 ug/ml) or control media for 24 hours, and then fixed the cells using 4% paraformaldehyde. When conducting ICC with the D3 and HMC3 co-culture we coated

the slides in accordance with D3 requirements and added the D3s, allowed them to attach overnight, and then added the HMC3 cells (1:1) and allowed them to attach for another 24 hours. Once the co-culture developed, we exposed the cells to DEP or control media for 24 hours before fixation. We followed ATCC's standard protocol for ICC fixation and completed the process by using a fluorescence microscope to image the fluorescent cells (See Appendix C).

P-gp was measured since it is the main focus of this study and is a known efflux transporter protein that is hypothesized to increase in both efflux action and protein production when exposed to DEP. The fluorescent imaging of P-gp will qualitatively distinguish between P-gp expression in control versus DEP exposed cells as well as establish the presence of P-gp on the endothelial cells.

In order to solidify the cell line we used as our model (D3), we also conducted ICC for both CD105 as well as ZO-1 which are indicators of endothelial cells. Endoglin, CD105, is a known glycoprotein found predominantly in vascular cell lineages, especially proliferating endothelial cells (Fonsatt1 et al., 2003). ZO-1 is a known protein component of human and rat endothelial cell tight junctions within the blood-brain barrier (Kubotera et al., 2019; Reinhold& Rittner, 2017; Tornavaca et al., 2015). It is indicated within the brain vasculature at the interendothelial junction between BBB specific endothelial cells (Watson et al. 1991).

The optimal standard for imaging ICC slides is with a confocal microscope, however, the resource was limited to the researcher of the thesis and instead a fluorescence microscope was used for imaging purposes.

Rhodamine-123 Accumulation Assay

The Rhodamine-123 Accumulation assay is a functional assay which is used for determining the activity of P-gp in a cell based on the accumulation of Rhodamine-123 within the cell. Rhodamine-123 is a light-sensitive fluorescent compound and therefore requires that this assay be completed in darkness. This assay was used for experiments regarding both a monoculture of endothelial cells and a co-culture of endothelial and microglial cells. The endothelial cells were seeded at 10,000 cells per cm² in dark, clear-bottom 96-well plates (Thermo Scientific #: 165305) and maintained in a 37°C, 5% CO₂ humidified incubator. The next day, the cells were dosed with either control media or DEP suspension (2000 ug/mL in 1% DMSO). A 1% DMSO solvent control and a positive control for P-gp inhibition, Tariquidar (100 uM) (Fisher Scientific#: NC0783015), were included in each plate as well (See complete procedures in Appendix D). The solutions in the wells were removed and the cells were rinsed to remove any excess Rho-123. The cells were then lysed by the addition of a 1:1 solution of DMSO:Ethanol, and fluorescence was measured using a spectrophotometer at 505/534 nm. In the case of the co-culture, endothelial cells are incubated for 24 hours, then the microglial cells are added, and both were allowed to incubate in a 37°C, 5% CO₂ humidified incubator for 24 hours before dosing. The remainder of the assay procedure is the same.

Inhibitor Optimization

Of particular interest with this specific accumulation assay was the continuous struggle we had with finding a negative or positive control that would work optimally and continuously over multiple trials. The initial Rhodamine-123 accumulation assay kit

provided recommended the use of Verapamil which is a known P-gp protein inhibitor (Fontaine et al., 1996). However, this is a generation one inhibitor and is thus not as specific to P-gp as newer compounds. The reason we found this to be unspecific to P-gp was its continued absence of significant data with each plate the inhibitor was used for. The determinant of whether the inhibitor worked properly or not was in its significant difference from the control group for each biological replicate. Within each biological replicate, we decided to omit the edges of the plates to account for the edge effect as well as randomly seed the plate to account for variability in cell suspension within the media.

Therefore, we attempted to find other inhibitors from literature and found that Zosuquidar, another known P-gp inhibitor, is a third-generation P-gp inhibitor and is thus meant to be more specific for P-gp inhibition (Jouan et al, 2016). However, we still observed inconsistent results, this was indicated by only some replicates having significant difference between the control group and the inhibitors that were intended to be the negative controls for the assay.

Thus, after ordering many third-generation P-gp inhibitors (Valspodar, Tariquidar, Vinblastine, and Elacridar) we conducted a comparative experiment to see which P-gp inhibitor would be most effective since all were stated as effective in literature (Jouan et al, 2016; Tai et al., 2009; Wang et al., 2018). Both Tariquidar (Fisher #NC0783015) and Elacridar (Selleckchem #S7772) showed significant differences from the control cells at 0.1 μ M and 10 μ M, respectively. Therefore, we decided to use Tariquidar at a 0.1 μ M concentration as our positive control for the Rho-123 accumulation assay. Tariquidar is also a known inhibitor of P-gp at three different binding sites in the transmembrane domain (Mollazadeh et al., 2018).

RNA Extraction, cDNA conversion, and RT-qPCR

To obtain quantitative data, we decided to conduct RT-qPCR on both the monoculture and co-culture when exposed to control media versus DEP dosed media. RT-qPCR allows you to evaluate the relative genetic expression of a target gene(s), relative to housekeeping (endogenously expressed) control gene(s). In order to obtain the genetic material used for RT-qPCR, we first had to extract RNA from the cell, convert the RNA to complementary DNA (cDNA), which was then used as our starting template for in RT-qPCR assay.

Briefly, we used the PureLink RNA Mini Kit (ThermoFisher 12183018A) for RNA extraction and purification from mammalian cells (See full procedure in Appendix E). The purified RNA was then aliquoted as 15 uL samples in three 0.2 mL RNase-Free microtubes plus an aliquot of ~5 uL for each sample to be measured for RNA yield and quality, using the Nanodrop spectrophotometer. The extracted RNA can be stored at -80°C until future use or it can be converted to cDNA immediately.

After the acquisition of purified RNA, the RNA was reverse transcribed into cDNA using the SuperScript™ IV VILO™ Master Mix with ezDNase™ Enzyme kit (Fisher 11766050) and following manufacturer's protocols. We utilized the reverse transcription protocol provided by Fisher for their SuperScript™ IV VILO™ Master Mix with ezDNase™ Enzyme kit (See full procedure in Appendix E). The volume of RNA needed was calculated using this equation: Vol. of RNA needed = 1000 ng/ estimated RNA concentration (Nanodrop measured), this way, all RNA samples will be standardized to 1 ug.

Next, the reverse transcriptase (RT) reaction mix is prepared (See full procedure in Appendix E). The primers are annealed by gently pipetting up and down the solution inside the reaction tubes while the tubes are removed from the ice and are incubated at room temperature for 10 minutes. After this period, the tubes are transferred to the 50°C-water bath where the reverse transcriptase will be at the optimal temperature to reverse transcribe the RNA. Next, the tubes are placed onto the heat block (at 85°C) for 5 minutes to inactivate the enzymes. The cDNA conversion is now complete and can either be stored undiluted in the -80°C freezer for the long term (months), in the -20°C for short-term storage (7 days), or it can be used immediately for qPCR amplification.

For the PCR amplification and RT-qPCR analysis, we utilized the ThermoFisher protocol, optimized by Bruce Lab. Before the actual PCR amplification can occur, we created an outline for our RT-qPCR Plate, designating the cDNA samples and the genes of interest, this can be done on a 96 well plate or a 384 well plate. Next, the cDNA samples must be diluted to either a 10x or 20x concentration, preferably 20x (See Appendix E for full procedure). Preparation of the PCR reaction matrix without cDNA requires the TaqMan™ Fast Advanced Master Mix (ThermoFisher 4444557), the TaqMan® Gene Expression Assays for both P-glycoprotein (Hs00184500_m1) and succinate dehydrogenase complex flavoprotein subunit A (SDHA) (Hs00188166_m1), a housekeeping gene, and finally nuclease-free water. Based on your number of reactions wells you can now prepare the TaqMan™ Fast Advanced Master Mix (2x), the corresponding TaqMan® Gene Expression Assay (20x), and nuclease-free water for a working solution in a 1.5 mL nuclease-free microtube. For each reaction well we will need an end volume of 20 uL, the PCR reaction mix without cDNA would require 1 uL

of the TaqMan® Gene Expression Assay (20x), 10 uL of the TaqMan™ Fast Advanced Master Mix (2x), and 4 uL of the nuclease-free water. The next step is to load the plate with the reaction mix, it is important to keep the plate on ice whilst completing this step.

For each gene of interest, we loaded the PCR reaction mix created earlier without the cDNA into each well (14 uL per well) designated for that specific gene of interest (following our plate outline). Then the 20x diluted cDNA samples were loaded for each technical replicate of that sample (biological sample). For each reaction well, we transferred 5 uL (12.5 ng total) into each of the wells designated for that specific biological cDNA sample. Once all outlined reaction wells were completed, we sealed the plate with its appropriate cover and placed it on ice until it was ready to run on the instrument. Finally, utilizing a QuantStudio 6 Real-time PCR system (ThermoFisher 4485691) the outline of the plate was uploaded and the plate assay was run.

This test was normalized by using SHDH a housekeeping gene that is known to not be related to the gene for P-gp; this was determined via a gene comparison matrix.

CHAPTER FOUR

Results

MTT (Cytotoxicity)

The MTT assay was first conducted to determine the concentration of DEP that would be sub-lethal to the cells at concentration below the extrapolated LC10. The MTT assay yielded the results of a single biological replicate, however the biological replicate (one plate with the same generation of cells) held 16 technical replicates for each group. The groups including a control group (0 $\mu\text{g/ml}$ DEP; HMC3 Media), and then groups dosed with increasing DEP concentrations at 5,000, 15,000, and 20,000 $\mu\text{g/ml}$ of DEP. This graph is a representation of the absorbance measured from the result of intracellular

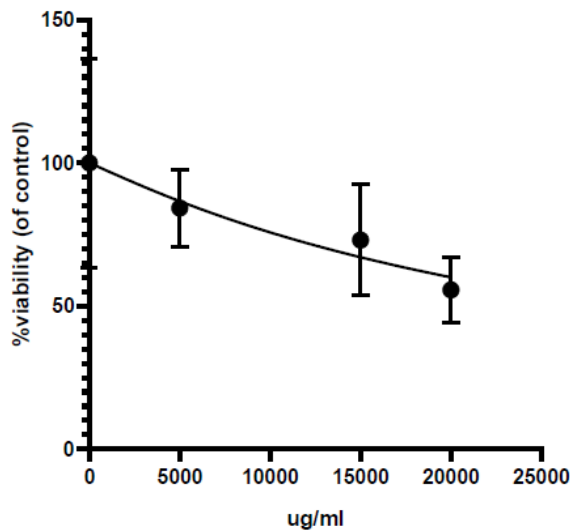


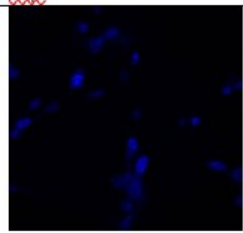
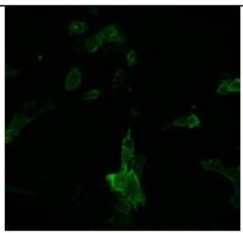
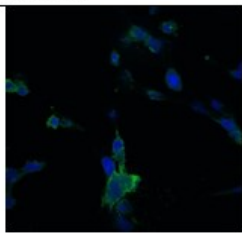
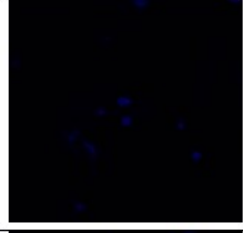
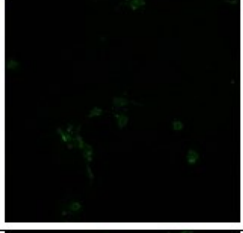
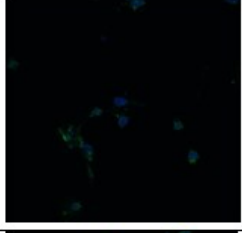
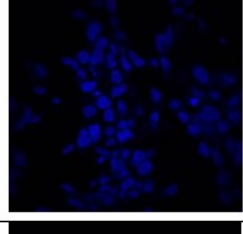
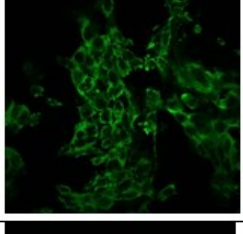
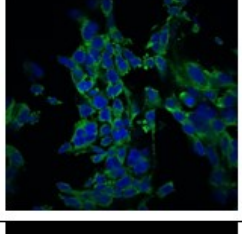
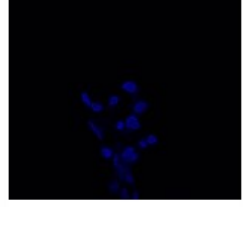
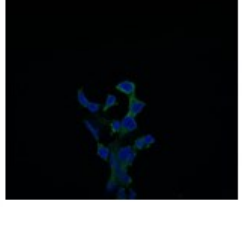
Figure 11: Concentration-Response Curve of DEP in hCMEC/D3s (24 hr. exposure)

NAD(P)H-dependent cellular oxidoreductase enzymes which reduce the MTT tetrazolium dye to an insoluble formazan form producing a bright purple color. This color

is then measured using an absorbance measuring tool. The lethal concentration 50% (LC50) of DEP in D3 cells was extrapolated to be 29,457 ug/mL due to the lack of the studies ability to reach the actual LC50 concentration. However, for our subsequent experiments, we chose to use a sublethal concentration of 2,000 ug/mL, which is lower than the extrapolated LC10, to ensure sublethal cellular responses.

Immunocytochemistry

The goal of fluorescent imaging is to qualitatively demonstrate the changes in cells via fluorescent antibodies that target specific structures in the cell.

Slide	Dapi	AF488	Combined
1. Mouse anti-CD105 (10 µg/mL) + Goat anti-Mouse AF488 (1:1000) + DAPI [4.5/3.5]			
2. Mouse anti-CD105 (10 µg/mL) + Goat anti-Mouse AF488 (1:1000) + DAPI [4.5/3.5]			
3. Rabbit anti-ZO1 (1:100) + Goat anti-Rabbit AF488 (1:1000) + DAPI [2.5/1.5]			
4. Rabbit anti-ZO1 (1:100) + Goat anti-Rabbit AF488 (1:1000) + DAPI [2.5/1.5]			

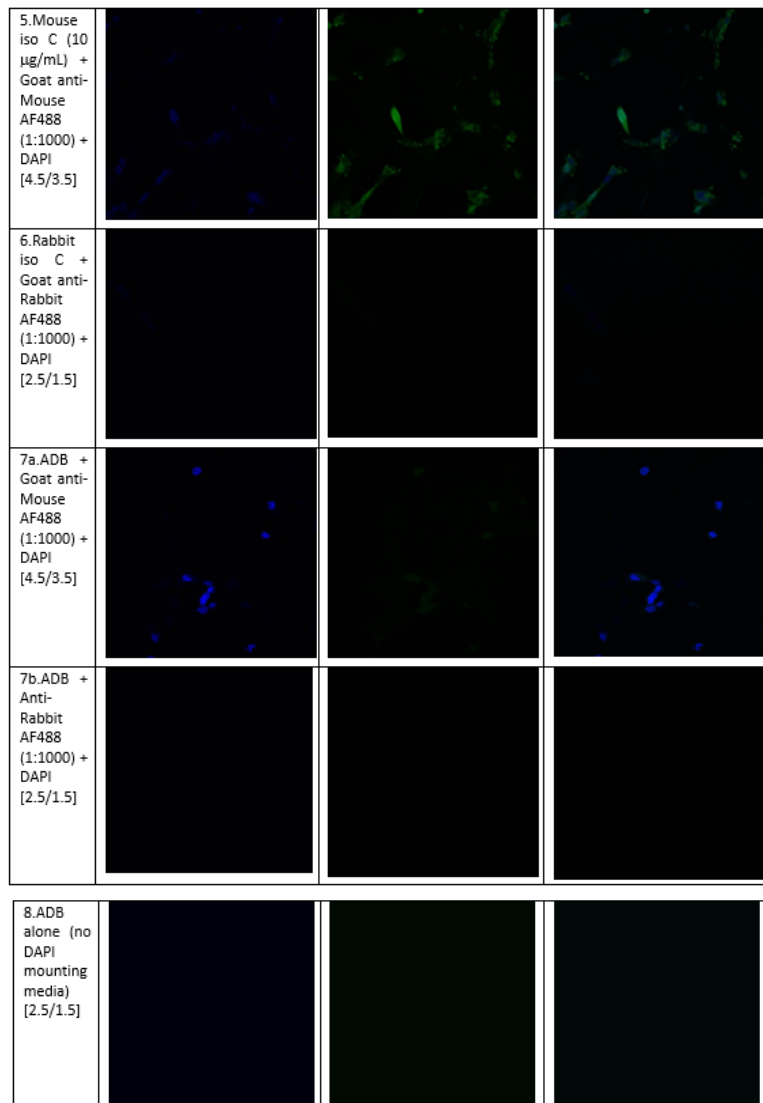


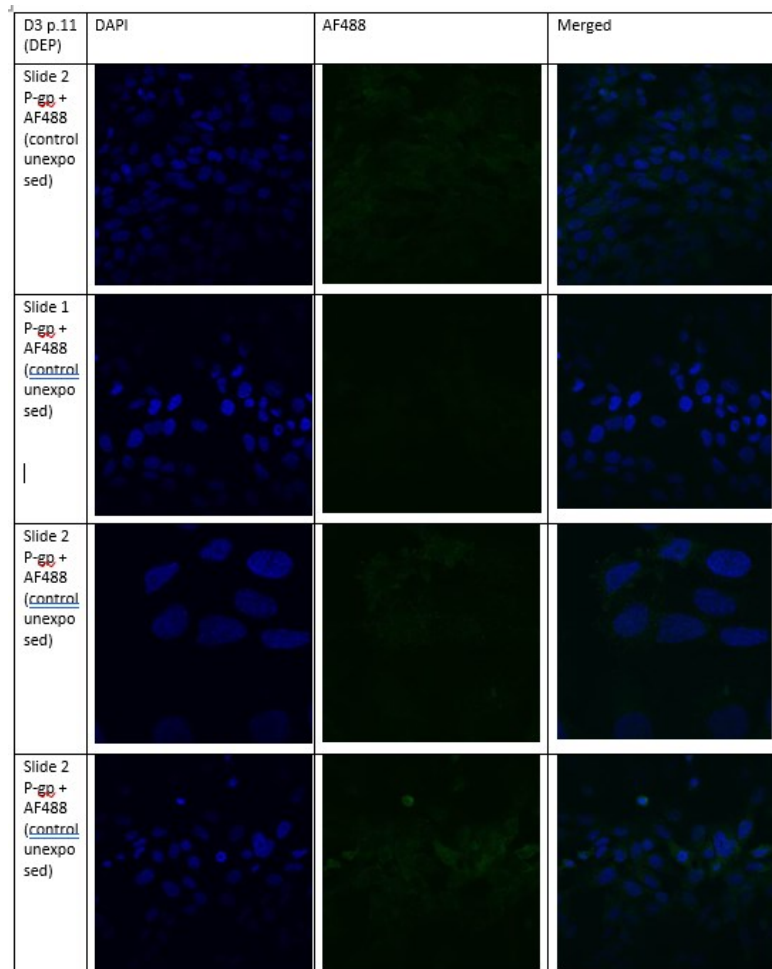
Figure 4 Figure 12: ICC Slides for ZO-1 and CD105, Fluorescence Microscopy, Taken in Bruce Lab

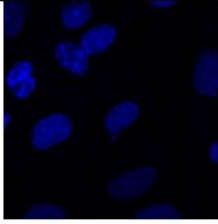
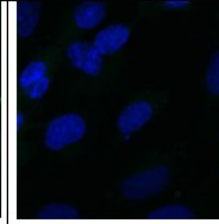
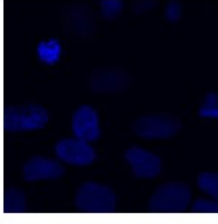
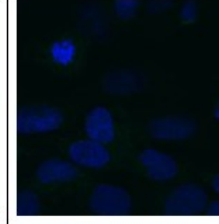
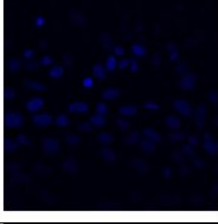
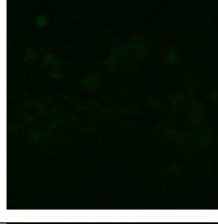
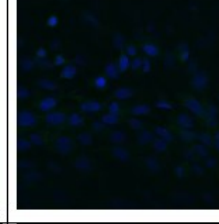
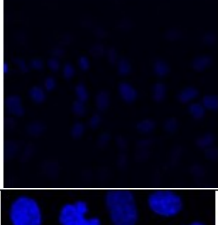
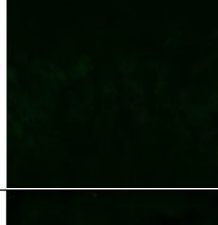
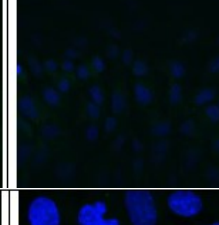
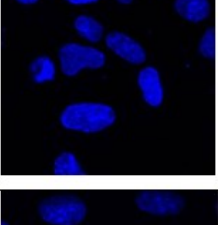
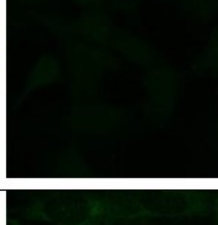
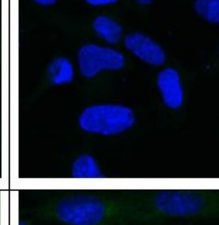
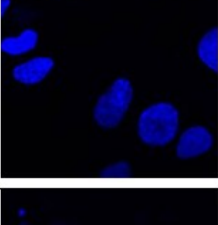
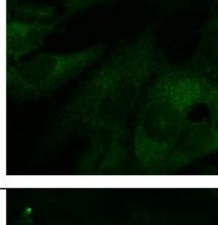
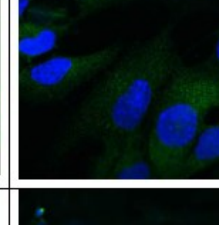
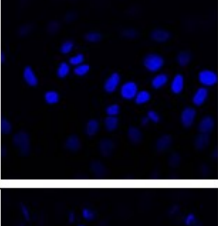
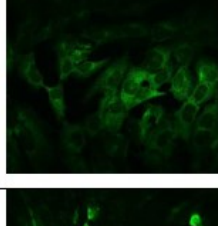
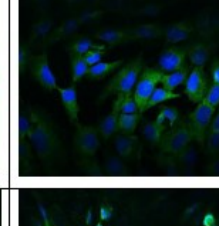
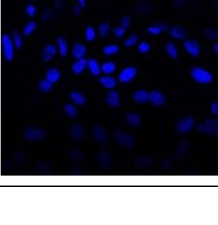
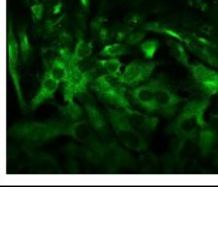
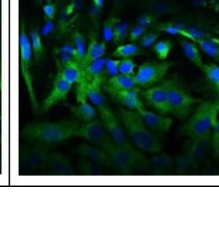
We needed to establish that our cell line (D3) was an accurate representative of the BBB endothelial cells. After staining for CD105 and ZO-1 we received these results indicating that our cells do produce both CD105 and ZO-1.

The above slide images demonstrate that without any antibodies there was no auto fluorescence seen; therefore, all fluorescence is from the cells only. We found that both

ZO-1 and CD105 were present in this line of endothelial cells thus contributing to their existence as endothelial cells of the BBB.

The goal of ICC in our experiment, was to visualize P-gp expression in the unexposed (control) and DEP-exposed D3 (BBB) monoculture. The nucleus of the cell is shown in blue (DAPI) and the P-gp membrane pump, is in green (AF488). The cells did exhibit autofluorescence, however, it can be noted that these cells do express p-gp since the cells in 1% DMSO fluoresce brightly and look similar to the expected fluorescence mentioned before for the known P-gp antibody.



Slide 3 P-gp + AF488 (DEP in 1% DMSO)			
Slide 3 P-gp + AF488 (DEP in 1% DMSO)			
Slide 3 P-gp + AF488 (DEP in 1% DMSO)			
Slide 3 P-gp + AF488 (DEP in 1% DMSO)			
Slide 6 ADB + AF488 (no exposur e)			
Slide 4 P-gp + AF488 (1% DMSO!! !)			
Slide 4 P-gp + AF488 (1% DMSO)			
Slide 4 P-gp + AF488 (1% DMSO)			

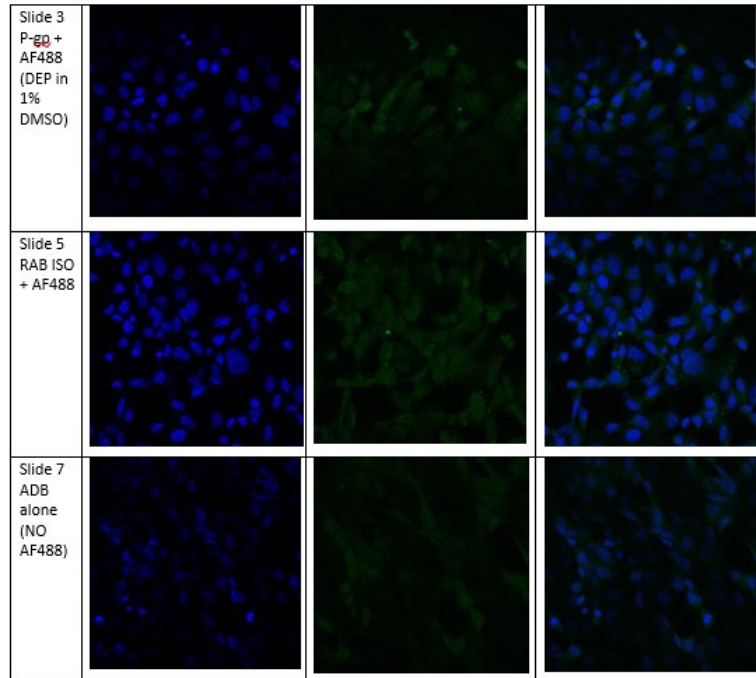


Figure 13: ICC Slides for P-gp, Fluorescence Microscopy, Taken in Bruce Lab

D3 cells without exposure to DEP demonstrate a light green fluorescence indicative of the presence of P-gp at what is considered normal expression. Cells which were acutely (24 hours) exposed to DEP showed only light fluorescence similar to a non-exposed cell. However, the endothelial cells exposed to the 1% DMSO control group showed increased expression of P-gp. This fluorescence is similar to the Abcam example shown earlier of cells possessing P-gp.

Rhodamine-123 Accumulation Assay

In this assay, we evaluated the effect of DEP exposure on P-gp activity in the D3 monoculture alone, and in co-culture. We normalized the data by dividing the average of the experimental fluorescence by the control groups fluorescence therefore demonstrating an increase or decrease in percentage of fluorescence in comparison to the control group. We further compared the monoculture's response to that of the co-culture after DEP exposure, to determine whether the presence of microglia altered P-gp activity under DEP exposure.

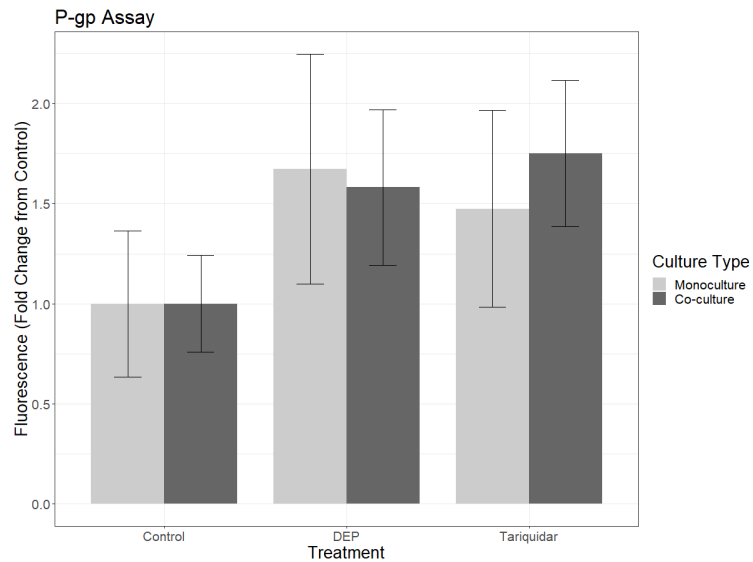


Figure 14: Rhodamine-123 accumulation assay demonstrates Rhodamine-123 accumulation that is inversely related to P-glycoprotein activity

Importantly to note, the accumulation of RHO-123 is inversely proportional to the activity of P-gp in the cell. Thus, the bars in Figure 14 indicate the amount of fluorescence and inversely the activity of P-gp. Under normal conditions, P-gp expels Rho-123 from the cell, resulting in limited intracellular RHO-123 accumulation. We completed six independent replicates (N = 6) of the accumulation assay for the monoculture of endothelial cells and six independent replicas (N= 6) for the co-culture.

Within each independent or biological replicant there was a measure of at least 16 technical replicates per group. To clarify, each plate (biological replicate) had 16 individual wells (technical replicates) with cells that were designated for each group, either control, DEP treated, or Tariquidar treated (Inhibitor). The DEP treated group and the group exposed to Tariquidar are not statistically different from the fluorescence measured for the control group.

Statistical Analyses: The data were first averaged across each plate to produce a single independent experiment per plate, for a total of 6 independent replicates ($N = 6$) for each treatment in each culture type. Fluorescence values for each cell culture group were scaled as fold increase from control. The non-parametric Mann-Whitney-U test was then used to test for differences between control and exposed conditions in each cell culture group and between the DEP-exposed conditions across cell culture groups. A Šidák correction was used to control for the family-wise error rate, yielding a p-value cutoff of 0.143.

The data found that there was no significant difference between any of the groups. However, trends can be observed, and it was found that cell exposed to DEP produced a similar fluorescent level as the cells exposed to Tariquidar, the known P-gp inhibitor.

Table 1: P-values of Mann-Whitney U Test for Rho-123 Accumulation Assay

p-values from Mann-Whitney U Test				
	Monoculture Control	Monoculture Exposed	Co-culture Control	Co-culture Exposed
Monoculture Control	0	0.2403	NA	NA
Monoculture Exposed	0.2403	0	NA	0.9372
Co-culture Control	NA	NA	0	0.3939
Co-culture Exposed	NA	0.9372	0.3939	0

This table further provides us with the understanding that, statistically, there is no significant data that arose from the Rho-123 Accumulation Assay.

RNA Extraction, cDNA conversion, and RT-qPCR

We extracted RNA and formulated the corresponding cDNA for 4 independent replicates of D3 monoculture unexposed (or control), 4 independent replicas of D3 monoculture acutely exposed to DEP, 3 independent replicas of the co-cultured epithelial cells and microglial cells without exposure (Control), and 3 independent replicas of the co-culture when acutely exposed to DEP. We then ran RT-qPCR specifically searching

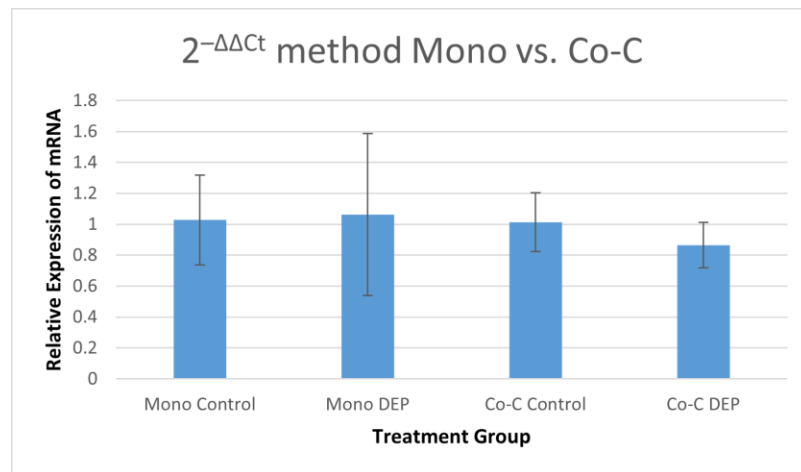


Figure 15: RT-qPCR Relative Gene Expression

for the P-gp gene and found that although none of the data was significant there were some interesting trends.

We used the $2^{-\Delta\Delta C_t}$ method utilizing a Welch's T-test to determine statistically significant differences between treatments and/or cell culture groups. Results indicated that there was no difference between the DEP-exposed groups and their corresponding control, or between the DEP-exposed monoculture and the DEP-exposed co-culture. As shown in Figure 15, the monoculture showed a similar P-gp expression after DEP exposure compared to the control monoculture. The co-culture, however, showed an interesting trend as the P-gp expression decreased after DEP exposure, compared to the control co-culture. These trends, however, are not significant, and more tests would need to be run to determine if there is any significant difference in the expression of P-gp by endothelial cells when exposed to DEP.

CHAPTER FIVE

Discussion

Immunocytochemistry

The results from immunocytochemistry of Z)-1 and CD105 contributes to the cell's structure as an endothelial cell of the BBB. The results of the P-gp fluorescent images showed that there was not a significant qualitative increase in P-gp expression in D3s after exposure to DEP, even though the cells do express P-gp (as shown by the increase in P-gp expression in the 1% DMSO group). This could indicate that DEP is not a promotor of P-gp expression in human BBB endothelial cells as previously hypothesized. What is interesting is the noticeable lack of increased P-gp expression that was mentioned by Hartz and collaborators in rat endothelial cells of the BBB that presented with increased expression of P-gp when exposed to DEP. This could indicate that the human endothelial cells react differently to DEP than rat endothelial cells.

In future studies it would be beneficial to examine the effects of DEP on endothelial cells at differing times during their exposure due to the fact that in a study of rat BBB endothelial and microglial cells there was biphasic effect, altering the expression of p-gp based on time and dose (Pan et al., 2011). However, since this study found the LC10 that was indicative of a sublethal dose of DEP, it would be more interesting to determine if time was a factor in P-gp expression. If it were, it could also contribute to a possible difference in acute and chronic DEP exposure. However, as we were limited to human cell models for this thesis, only acute exposure (24 hours) could be theorized.

Another area of interest for ICC staining of P-gp would be the use of a confocal microscope. The confocal microscope is the ideal imaging modality for ICC-stained slides. However, the technology was unavailable to the researcher and could allow future researchers to elaborate on the findings of this thesis.

Rhodamine-123 Accumulation Assay

Although the results of the Rhodamine-123 Accumulation assay were not significant, it still demonstrated an increasing trend with the accumulation of fluorescent Rhodamine-123 which is inversely related to P-gp activity, thus indicating a decreasing trend in P-gp activity as the cells are exposed to DEP. Interestingly, contrary to our hypothesis, P-gp activity showed a decreasing trend in both the monoculture and co-culture after DEP exposure; however, the trend was not significantly significant. This could possibly suggest that DEP could contribute to the inhibition of molecular efflux. It could also be posited that DEP does not affect P-gp but rather a different efflux pump of the endothelial cell causing the trend of increased cellular fluorescence during the Rhodamine-123 assay. It would be of interest to future studies to determine if DEP affects other transportation proteins within endothelial cells of the BBB.

The findings of Hartz and colleagues demonstrated an increase in P-gp function when rat endothelial cells were exposed to DEP (Hartz et al., 2008). This could again correlate to a difference between human and rat endothelial cell reactions to DEP, however, further research would have to be conducted to determine significance of the trends observed in this research.

The optimization of the Rhodamine-123 assay should also be noted here since the data shows no overall significance. However, at each biological replicate, meaning each

plate completed, the data was significantly different between the control group and the inhibitor Tariquidar, our negative control. The data became insignificant once statistics was used on the compilation of all biological replicates and the standard errors of each group expanded.

RT-qPCR (Relative Gene Expression)

The RT-qPCR data was somewhat differential in nature as the exact mechanisms of microglial and endothelial exchange is not fully understood. The D3 monoculture showed no significant difference in P-gp expression after exposure to DEP. This could indicate that there is not an increase or decrease in transcription of the P-gp gene when exposed to DEP. This could also contribute to a possibility DEP has no effect on the modulation of DNA, however, future studies to determine the exact route of DEP activity within the cell would need to be studied and that is outside the reach of this thesis paper. The slight decreasing trend of P-gp expression seen in the co-culture of endothelial and microglial cells could possibly contribute to the idea that DEP causes microglial cell activation, which in turn could affect endothelial protein expression and function. However, since the data was not significant, no definitive conclusions can be derived from the data. In future research it would be interesting to use a MAGPIX assay which could demonstrate the definitive presence of microglial proinflammatory cytokines known to affect endothelial cells.

Conclusion

The significance of this study was in its novelty, as there has not been any research conducted, to our knowledge, of the effect of DEP exposure on the p-glycoproteins of human BBB endothelial cells as a monoculture and in a co-culture, in

vitro setting with microglia. Although previous studies found an up-regulation in p-glycoprotein in rat cells, the same could not be said for human endothelial (D3) cells.

The monoculture of human endothelial cells alone demonstrated a decreasing trend in P-gp activity via the Rhodamine-123 accumulation assay, where the data showed an increased trend of accumulation compared to the control group, indicating a possible decrease in P-gp activity. However, since the data was not significant, it is merely a postulation and would need to be confirmed by completing more biological replicates of the Rhodamine-123 assay, thus potentially decreasing the standard error of the groups, providing significance to the model. The possible decrease of P-gp could be attributed to DEP rendering the protein inactive even though they are present in the cells. This would require future research into DEP's binding at p-glycoprotein and whether it does in fact bind to P-gp or if it is instead binding to another efflux protein found in human endothelial cells. The dysfunction of endothelial BBB cells associated with the inhibition of efflux proteins is a known tributary to neurodegenerative diseases (). Thus, it would be beneficial to research further the trends found in the function of export proteins when exposed to DEP.

We theorize that although there was not a significant increase in P-gp expression at 24 hours, the cells could be exhibiting a different reaction at differing times of exposure and suggest that future studies seek to determine if DEP causes a time-dependent reaction associated with the alteration of P-gp expression or function.

The co-culture consisting of human endothelial and human microglial cells showed a decreasing trend in P-gp activity as well, though to a lesser extent than the monoculture, when exposed to the Rhodamine-123 accumulation assay. This finding,

combined with the trend of downregulation in P-gp gene expression (shown in the RT-qPCR Assay) demonstrates a possible effect of microglial influence on endothelial cells that is yet undiscovered or unknown. This could be an interesting point for further research and could contribute to our understanding of how the BBB dysfunction can alter the pathogenesis of neurodegenerative diseases. It would be of interest to future researchers to complete a MAGPIX assay to determine what cytokines are being expressed by microglial cells when they are exposed to DEP. It would also be important to integrate the concept of time-dependent reactions as microglia are known to become activated and produce cytokines at differing times after their initial exposure to foreign molecules (Kreutzberg, 1996; Lui & Hong, 2003; Pan et al., 2011).

This thesis hypothesized that after acute exposure to DEP, there would be increased expression and function of P-gp in endothelial cells as a monoculture. This was not supported by the research completed in this thesis. The ICC staining for P-gp in the endothelial cells demonstrated that there was not an increase in P-gp expression qualitatively and the RT-qPCR demonstrated that there was not a significant difference in P-gp expression in the monolayer exposed to DEP than in the control group. It was also found that there was no significant difference in P-gp function when exposed to DEP, however, there was a trend that indicated P-gp could play some role in inhibiting efflux of Rhodamine-123 out of the cell. This again could be further expanded upon by completing more biological replicates to increase the overall size of the experiment and thus decrease the standard error bars to a significant level. Or more tests could further prove its insignificance and solidify the findings of this thesis.

This thesis also hypothesized at DEP exposure to a co-culture of endothelial and microglial cells would induce increased expression of P-gp but decreased functionality due to microglial cytokine disruption. Not only did the co-culture not have a significant difference in P-gp gene expression in RT-qPCR, but there was also a decreased trend in P-gp expression. This could be caused by a cytokine induced mechanism that affects the production of efflux proteins, however, there is not data in this thesis to prove this postulation and thus more research would need to be conducted. However, future research regarding MAGPIX could evaluate the cytokines produced by microglial cells upon their introduction to DEP and determine if those cytokines have any effect on the expression of efflux proteins.

Lastly, it was hypothesized that DEP exposure would induce a similar effect on P-gp expression and function in both the monoculture as well as the co-culture. This hypothesis proved to be correct because there was no significant difference in either the monoculture or co-cultures P-gp function or expression.

APPENDICES

APPENDIX A

Cell Culture

The EndoGRO complete media from EMD Millipore (Product number: SCME004), consisted of basal medium supplemented with EndoGRO-L`12S Supplement (1 ml), Fetal Bovine Serum (FBS) (5%), Hydrocortisone (1 ug/ml), Ascorbic Acid (50 ug/ml), rhEGF (5 ng/ml), Heparin (50 ug/ml), L-glutamine (10 mM), and Penicillin-Streptomycin (1%) from ThermoFisher (product number: 15140122). The cells, which are stored in a vial kept in liquid nitrogen, can be thawed using the recommended Millipore protocol for thawing of the hCMEC/D3 cell line. The cells are then maintained in a T-75 flask containing 10-12 mL of EndoGRO complete media while placed in a 37°C, 5% CO₂ humidified incubator. The cells are monitored daily for confluency and imaged at the 5x and 10x levels in order to view overall growth and cellular anatomy respectively. Their media may be changed 2-3 times a week, always using sterile techniques in a hood. Once the cells reach 80% to 100% confluency then the cells are split using sterile techniques.

The cell media is removed, they are washed with PBS (ThermoFisher #14190144), and are then dissociated from the flask using 2.5 mL of TrypLE™ Select Enzyme from ThermoFisher (Product number: 12563011) and incubating in a 37°C, 5% CO₂ humidified incubator for 4 minutes, the cells are then lightly wacked and viewed under the microscope to ensure dissociation from the flask surface. After this, the TrypLE is neutralized by the addition of 7.5 mL of Dulbecco's Modified Eagle's Medium (DMEM) purchased from Sigma-Aldrich (Product #: D6429-1L) and placed into a 15 mL

centrifuge tube. The cells are counted, to do this, about 11 uL of suspended cells are added to 11 uL of Thiazolyl Blue Tetrazolium Blue (Product #: M5655-1G), a color indicator of cell viability, and are loaded into a dual slide specific to the ThermoFisher Countess II Automated Cell Counter (hemocytometer) where the cell count and viability are measured. The 15 mL centrifuge tube is then centrifuged at 300 x g for 5 minutes to pellet the cells. The supernatant is discarded, and the cells are resuspended in EndoGRO complete media at 1 million cells per mL media concentration. The cells are then subcultured and are either frozen back for storage using 10% DMSO and slow-freeze (1 degree per min) containers, or they are added to new flasks/ plates to form the next passage.

The immortalized human microglial cells, HMC3s, were purchased from ATCC (Product #: CRL-3304) and were maintained in an HMC3 media consisting of 450 mL Eagle's Minimum Essential Media (EMEM) (ATCC #30-2003), Fetal Bovine Serum (FBS, 10%) from Fisher Scientific (#MT35011CV), and Penicillin-Streptomycin (1%). The cells that are received are either stored in liquid nitrogen or are placed in a T-75 flask for their cell line continuation in accordance with the company's recommended procedure. The flasks are kept in a 37°C, 5% CO₂ humidified incubator and are imaged daily, their media can be changed 2-3 times a week in hoods using a sterile technique. Once the cells reach a maximum of 3 million cells they will need to be sub-cultured. In a hood, while using sterile technique, the cell's media is removed and the cell's surface is rinsed with PBS, 2-3 mL of TripLE is added to the flask and it is incubated for 5 - 15 minutes. After the incubation period it is important to NOT wack the flask as it will cause clumping of the cells. Instead, add 6-8 mL of complete HMC3 medium and aspirate by

gently pipetting. The new cultures should be in accordance with guidelines, ensuring a concentration between 1×10^4 and 4×10^4 viable cells/cm², but not exceeding 7×10^4 cells/cm². Cells may also be frozen back using the same method as the D3 cells listed above.

The DEP suspension was produced as a 2 mg/ml (2000 ug/ml) stock solution concentration. Briefly, 0.02 g of SRM2975 (NIST standard DEP) was added to 10 mL of PBS++ or water (or dosing media, no FBS). This suspension is vortexed for 1 minute, then sonicated for 45 minutes utilizing an ultrasonicator, before it is warmed for 15 minutes in the 37°C-water bath. Before this media can be used on cells was sequentially filtered using various filter sizes down to 0.45 µm filter, to obtain fine DEP. This media is then ready for use and can be used immediately or kept in the 4°C for up to 2 weeks.

APPENDIX B

MTT

The purple color is measured using a spectrophotometer at 595 nm, with 650 nm as a reference wavelength, and the absorbance is proportional to the number of viable cells. We plotted absorbance against concentration to determine the IC50 and IC10 of DEP, using both D3 (endothelial cells) and the HMC3 (microglial cells). The cells grown in a 96-well plate are exposed to increasing concentration of DEP suspension (0 , 5000, 15000, 18000, 20,000 ug/ml) for 22-24 hours. After the 22-24 hour incubation period, 5 mg/ml MTT dye is added directly to the cell culture media and the cells are incubated for 2-4 additional hours. At the end of the incubation, all solutions in the wells are removed and the remaining cells are lysed using DMSO: Ethanol (1:1) solution, which solubilizes the formazan product. The plate is then incubated at room temperature while on a plate shaker (at approximately 200 rpm) for 10 minutes. Last, the plate's absorbance is then measured at the 595-650 nm wavelength.

APPENDIX C

Immunocytochemistry

Before the process of immunocytochemistry can begin, the cells must be grown on glass slides. These glass slides however are not optimal for cell growth without the use of coatings to allow cells to attach and form a cellular matrix. Microglial cells, HMC3's alone, require Poly-D-Lysine coated slides; 5 mg of Poly-D-Lysine purchased from Sigma-Aldrich (P7280) is combined with 50 mL of nanopure water and stored in a polypropylene vial at 4°C. Dilute 1 mL of this stock solution into 9 mL of nanopure water, spread the appropriate amount of solution (in this case 500 uL) in each slide chamber, and allow it to cover the entire surface of the culture piece. From this point, the slides can be incubated at room temperature for 3 hours, at 37°C for 1 hour, or 4°C overnight or up to one week. However, as soon as the slides are to be used it is important to remove excess solution and wash the slide with sterile PBS or DMEM/F-12 + HEPES before seeding cells onto the slides.

Endothelial cells, D3's, also require the glass slide to be coated with bovine collagen solution (1:20 dilution in PBS-free) (Millipore #: C4243-20ml) and incubator at 37 dC for at least one hour. Before their use, the collagen solution is removed from the chambers and each chamber is rinsed with PBS-free before the addition of D3 seeded at 5,000 to 10,000 cells per cm². The cells are then maintained in the 37°C, 5% CO₂ humidified incubator. Briefly, 24 hours after cells were seeded on glass slides, we exposed the cells to DEP (2000 ug/ml) or control media for 24 hours, and then fixed the cells using 4% paraformaldehyde. When conducting ICC with the D3 and HMC3 co-

culture we coated the slides in accordance with D3 requirements and added the D3s, allowed them to attach overnight, and then added the HMC3 cells (1:1) and allowed them to attach for another 24 hours. Once the co-culture was developed, we exposed the cells to DEP or control media for 24 hours before fixation.

Briefly, we followed ATCC's standard protocol for ICC: First, we fixed the cells using 4% PFA for 15 min at room temperature, rinsed cells 3 times in 0.02M PBS-free, used 10% BSA blocking for 45 min to block cells, and then added the primary antibody against P-gp (Rabbit monoclonal anti-Pgp; ABCAM, Ab235954) at a 1:100 dilution and incubated overnight in 4 dC protected from light. The next day, the primary antibody solution was removed, and cells were rinsed 3 times with 0.2M PBS-free. The secondary antibody (Goat anti-Rabbit AF488, ABCAM, Ab150081) was then added at 1:1000 dilution and incubated at room temperature for 1.5 hours. Finally, cells were counterstained with DAPI (nuclear stain) for 5 minutes and then the coverslip was mounted using Diamond Prolong Antifade Mounting Media (Invitrogen P36961).

APPENDIX D

Rhodamine-123 Accumulation Assay

The endothelial cells were seeded at 10,000 cells per cm² in dark, clear-bottom 96-well plates (Thermo Scientific #: 165305) and maintained in a 37°C, 5% CO₂ humidified incubator. The next day, the cells were dosed with either control media or DEP suspension (2000 ug/mL in 1% DMSO). A 1% DMSO solvent control and a positive control for P-gp inhibition, Tariquidar (100 uM) (Fisher Scientific#: NC0783015), were included in each plate as well. The cells were incubated in 37°C, 5% CO₂ humidified incubator for another 24-hours. After dosing overnight, we remove 50 uL and store this for MAGPIX analysis, to the remaining 50 uL of solution in each well of the 96 well plate, we add 100 uL of Rhodamine-123 (Sigma-Aldrich #: 83702), and since Rho-123 is a light-sensitive fluorescent we wrap the plates in aluminum foil to avoid light exposure. The cells are then incubated in a 4°C refrigerator for 1 hour. Afterwards, the plate was incubated at 37°C, 5% CO₂ humidified incubator for an additional hour. Last, the solutions in the wells were removed and the cells were rinsed twice with PBS-free to remove any excess Rho-123. The cells are then lysed by the addition of a 1:1 solution of DMSO:Ethanol, and fluorescence is measured using a spectrophotometer at 505/534 nm. In the case of the co-culture, endothelial cells are incubated for 24 hours, then the microglial cells are added, and both are allowed to incubate in a 37°C, 5% CO₂ humidified incubator for 24 hours before dosing. Then the rest of the assay procedure is the same.

APPENDIX E

RNA Extraction, cDNA conversion, and RT-qPCR

To obtain quantitative data, we decided to conduct RT-qPCR on both the monoculture and co-culture when exposed to control media versus DEP dosed media. RT-qPCR allows you to evaluate the relative genetic expression of a target gene(s), relative to housekeeping (endogenously expressed) control gene(s). In order to obtain the genetic material used for RT-qPCR, we first had to extract RNA from the cell, and convert the RNA to complementary DNA (cDNA), the cDNA was then used as our starting template for RT-qPCR.

Briefly, we used the PureLink RNA Mini Kit (ThermoFisher 12183018A) for RNA extraction and purification from mammalian cells. Once the T-75 flask of D3 only or D3 with HMC3 cells was at least 70% confluent, we performed RNA extraction. During the initial phase of the process, the cell media is removed, and the cells are washed with PBS, the PBS is then removed, and the cells are lysed using a prepared lysing buffer containing 1mL lysis buffer (provided in the kit) in 10 mL of 1% 2-mercaptoethanol (ThermoFisher 21985023). Then 0.6 mL of the prepared lysis buffer is added to the T-75 flask with cells and the buffer is pipetted until the cells seem lysed (will appear clear but viscous). The lysed cells and solution are then transferred into a Homogenizer inserted in a microcentrifuge Collection Tube and are placed into a centrifuge and run at 12,000 x g for 2 minutes at room temperature. After this, keep the remaining solution in the collection tube but discard the homogenizer insert. The same volume of 70% Ethanol (0.6 mL) is added to the remaining cell solution in a 1:1 ratio,

however, if any of the sample's volume was lost during the homogenization step it is important to adjust the volume of 70% ethanol added. Vortex the sample with the 70% ethanol to homogenize then transfer 700 uL of the sample to a new spin cartridge inside of a collection tube. Centrifuge the sample at 12,000 x g for 15 seconds at room temperature (RT) and discard any flow through in the collection tube. Repeat the process of adding the sample + ethanol mixture to the same spin cartridge and collection tube and run the remaining mixture in the centrifuge for 15 seconds at 12,000 x g at RT. Next, we utilized the On-column PureLink DNase Treatment to ensure there was no genomic DNA in the sample. In order to complete this, 350 uL of Wash Buffer I (from the kit) is added to the spin cartridge containing the bound RNA and it is again centrifuged for 15 seconds at 12,000 x g at RT. However, once the sample is complete, we discard the flowthrough and collection tube. The spin cartridge gets inserted into a new collection tube and 80 mL of PureLink DNase mixture is added directly onto the surface of the spin cartridge membrane where it incubates for 15 minutes at RT. The PureLink DNase mixture is composed of 8 uL of 10X DNase I Reaction Buffer (in the kit), 10 uL of Resuspended DNase (~3U/uL) (aliquoted and stored in -20°C) (in the kit), and 62 uL of RNase Free Water (in the kit) for a final volume of 80 uL (per cell sample). After the 15-minute incubation, 350 uL of Wash buffer I is added to the spin cartridge, and the sample is centrifuged at 12,000 x g for 15 seconds at RT, the flowthrough and collection tube are discarded after, and the spin cartridge is inserted into a new collection tube. 500 uL of Wash Buffer II (in the kit, but reconstituted in ethanol) is added to the spin cartridge and is centrifuged at 12,000 x g for 15 seconds at RT. The flowthrough is discarded but the collection tube is kept and 500 uL of Wash Buffer II is again added and centrifuged out.

After the flowthrough is discarded reinsert the spin cartridge into the collection tube and centrifuge the empty spin cartridge at 12,000 x g for 1 minute at RT in order to dry the RNA bound membrane. After the drying cycle, remove the flowthrough and collection tube and insert the spin cartridge into a recovery tube. Add 30-100 uL (we used 55 uL) RNase-free water to the center of the spin cartridge and incubate for 1 minute before centrifuging at >12,000 x g for 1 minute at RT to elute the RNA from the membrane and into the recovery tube. The purified RNA is then aliquoted as 15 uL samples in three 0.2 mL RNase-Free microtubes plus an aliquot of ~5 uL for each sample to be measured for RNA yield and quality, be sure to bring an additional aliquot of the RNase-Free water from earlier to calibrate the Nanodrop spectrophotometer that the RNA samples are tested on. The extracted RNA can be stored at -80°C until future use or it can be converted to cDNA immediately.

After the acquisition of purified RNA, the RNA was reverse transcribed into cDNA using the SuperScript™ IV VILO™ Master Mix with ezDNase™ Enzyme kit (Fisher 11766050) and following manufacturer's protocols. We utilized the reverse transcription protocol provided by Fisher for their SuperScript™ IV VILO™ Master Mix with ezDNase™ Enzyme kit. Before beginning the process of cDNA conversion, it is important to prepare heating devices and cooling techniques, this includes setting a water bath to 50°C, heating the heating block to 85°C, and preparing an ice container to place tubes containing RNA or cDNA. After this initial set up the purified RNA samples are removed from the -80°C freezer and placed onto ice where we will prepare the gDNA digestion reaction mix. For each RNA sample to be transcribed, prepare one reverse transcriptase (RT) reaction tube and optionally one no reverse transcriptase (NoRT)

reaction tube, this is to ensure that the RNA sample that does not receive reverse transcriptase is not being transcribed into cDNA. In the RT reaction tube, a RNase-Free 0.2 microtube, that is sitting on ice, prepare 10 uL gDNA digestion reaction mix with the following components: 1 uL 10X ezDNase Buffer + 1 uL ezDNase Enzyme + Volume of RNA needed (e.g., 2 uL for our samples) + [10 - (1+1+2)] uL of Nuclease-free water (for a total of 10 uL solution). The volume of RNA needed can be calculated using this equation: Vol. of RNA needed = 1000 ng/ estimated RNA concentration (Nanodrop measured), this way, all RNA samples will be standardized to 1 ug. After the creation of the gDNA digestion reaction mix, mix gently but do not vortex, then move the mix from the ice to the incubator (37°C) for 2 minutes to allow for the digestion to occur. After the incubation period, the microtubes should be centrifuged to allow all liquid to return to the bottom of the tube and place the microtubes back onto the ice. Next, the reverse transcriptase (RT) reaction mix is prepared, this is done by adding either 4 uL of SuperScript IV VILO Master Mix and 6 uL of Nuclease-free water to the RT reaction tube or 4 uL of SuperScript IV VILO No RT Control and 6 uL Nuclease-free water to the NoRT reaction tube while they remain on ice. Next, the primers are annealed by gently pipetting up and down the solution inside the reaction tubes while the tubes are removed from the ice and are incubated at room temperature for 10 minutes. After this period, the tubes are transferred to the 50°C-water bath where the reverse transcriptase will be at the optimal temperature to reverse transcribe the RNA. Next, the tubes are placed onto the heat block (at 85°C) for 5 minutes to inactivate the enzymes. The cDNA conversion is now complete and can either be stored undiluted in the -80°C freezer for the long term

(months), in the -20°C for short-term storage (7 days), or it can be used immediately for qPCR amplification.

For the PCR amplification and RT-qPCR analysis, we utilized the ThermoFisher protocol, optimized by Bruce Lab. Before the actual PCR amplification can occur, one needs to create an outline for their RT-qPCR Plate designating the cDNA samples and the genes of interest, this can be done on a 96 well plate or a 384 well plate. Next ice must be prepared for items that thaw on ice. Next, the cDNA samples must be diluted to either a 10x or 20x concentration, preferably 20x. For the more commonly used 20x dilution, add 20 μL (1000ng, 50 ng/ μL) of cDNA stock to 380 μL of Nuclease-free water, this will yield a working solution of 2.5 ng/ μL for the cDNA sample. Briefly vortex the tube and gently centrifuge the tube to return the sample to the bottom of the tube. Preparation of the PCR reaction matrix without cDNA requires the TaqMan™ Fast Advanced Master Mix (ThermoFisher 4444557), the TaqMan® Gene Expression Assays for both P-glycoprotein (Hs00184500_m1) and succinate dehydrogenase complex flavoprotein subunit A (SDHA) (Hs00188166_m1), a housekeeping gene, and finally nuclease-free water, all kept on ice. Gently resuspend the solutions by vortexing and briefly centrifuging to return the solution to the bottom of the tube. Next, determine the number of reactions needed for each TaqMan® Gene Expression Assay, Applied Biosystem recommends using 4 replicates, but 2 to 3 is acceptable. For each gene of interest, the number of reaction wells is equal to your number of biological replicates times the number of technical replicates per sample times the number of experimental groups. For example, if you have 4 biological samples ($N=4$) and Taqman suggests 3 technical replicates per sample ($n=3$ /triplicates) plus you have four experimental groups ($n=4$),

then for the Taqman Gene Expression Assay, you will need $3 \times 4 \times 4 = 48$ reaction wells. Based on your number of reactions wells you can now prepare the TaqMan™ Fast Advanced Master Mix (2x), the corresponding TaqMan® Gene Expression Assay (20x), and nuclease-free water for a working solution in a 1.5 mL nuclease-free microtube. For each reaction well we will need an end volume of 20 uL, the PCR reaction mix without cDNA would require 1 uL of the TaqMan® Gene Expression Assay (20x), 10 uL of the TaqMan™ Fast Advanced Master Mix (2x), and 4 uL of the nuclease-free water. On the scale of our example, we would most likely prepare enough solution not for exactly 48 reaction wells, but for 50 reaction wells in order to account for volume loss. In that instance, we would require 50 uL of the TaqMan® Gene Expression Assay (20x), 500 uL of the TaqMan™ Fast Advanced Master Mix (2x), and 200 uL of the nuclease-free water. Then mix the solution and centrifuge briefly. The next step is to load the plate with the reaction mix, it is important to keep the plate on ice whilst completing this step. For each gene of interest, load the PCR reaction mix created earlier without the cDNA into each well (14 uL per well) designated for that specific gene of interest (follow your plate outline). Then the 20x diluted cDNA samples can be loaded for each technical replicate of that sample (biological sample). For each reaction well, transfer 5 uL (12.5 ng total) into each of the wells designated for that specific biological cDNA sample. Once all outlined reaction wells are completed, seal the plate with its appropriate cover and place it on ice until it is ready to run on the instrument. Finally, utilizing a QuantStudio 6 Real-time PCR system (ThermoFisher 4485691) the outline of the place can be uploaded and the plate assay can be run.

BIBLIOGRAPHY/ REFERENCES

- Abbott, N., Rönnbäck, L. & Hansson, E. Astrocyte–endothelial interactions at the blood–brain barrier. *Nat Rev Neurosci* 7, 41–53 (2006). <https://doi.org/10.1038/nrn1824>
- Abu-Qare AW, Elmasry E, Abou-Donia MB. A role for P-glycoprotein in environmental toxicology. *J Toxicol Environ Health B Crit Rev.* 2003 May-Jun;6(3):279-88. DOI: 10.1080/10937400306466. PMID: 12746142.
- Adar, S.D., Filigrana, P.A., Clements, N. et al. Ambient Coarse Particulate Matter and Human Health: A Systematic Review and Meta-Analysis. *Curr Envir Health Rpt* 1, 258–274 (2014). <https://doi.org/10.1007/s40572-014-0022-z>
- Alliot F, Godin I, Pessac B. Microglia derive from progenitors, originating from the yolk sac, and which proliferate in the brain. *Brain Res Dev Brain Res.* 1999 Nov 18;117(2):145-52. DOI: 10.1016/s0165-3806(99)00113-3. PMID: 10567732.
- “Basic Principles of RT-QPCR.” Thermo Fisher Scientific - US, www.thermofisher.com/us/en/home/brands/thermo-scientific/molecular-biology/molecular-biology-learning-center/molecular-biology-resource-library/spotlight-articles/basic-principles-rt-qpcr.html.
- Best, E. A., Juarez-Colunga, E., James, K., LeBlanc, W. G., & Serdar, B. (2016). Biomarkers of Exposure to Polycyclic Aromatic Hydrocarbons and Cognitive Function among Elderly in the United States (National Health and Nutrition Examination Survey: 2001-2002). *PloS one*, 11(2), e0147632. <https://doi.org/10.1371/journal.pone.0147632>
- Block, M. L., Wu, X., Pei, Z., Li, G., Wang, T., Qin, L., Wilson, B., Yang, J., Hong, J. S., & Veronesi, B. (2004). Nanometer size diesel exhaust particles are selectively toxic to dopaminergic neurons: the role of microglia, phagocytosis, and NADPH oxidase. *FASEB journal: official publication of the Federation of American Societies for Experimental Biology*, 18(13), 1618–1620. <https://doi.org/10.1096/fj.04-1945fje>
- Boje KM and Arora PK (1992) Microglial-produced nitric oxide and reactive nitrogen oxides mediate neuronal cell death. *Brain Res* 587:250–256.
- Boland, S., Baeza-Squiban, A., Fournier, T., Houcine, O., Gendron, M., Chévrier, M., . . . Marano, F. (1999). Diesel exhaust particles are taken up by human airway epithelial cells in vitro and alter cytokine production. *American Journal of Physiology-Lung Cellular and Molecular Physiology*, 276(4). doi:10.1152/ajplung.1999.276.4.1604

- Brook RD, Franklin B, Cascio W, Hong Y, Howard G, Lipsett M, Luepker R, Mittleman M, Samet J, Smith SC Jr, Tager I; Expert Panel on Population and Prevention Science of the American Heart Association. Air pollution and cardiovascular disease: a statement for healthcare professionals from the Expert Panel on Population and Prevention Science of the American Heart Association. *Circulation*. 2004 Jun 1;109(21):2655-71. DOI: 10.1161/01.CIR.0000128587.30041.C8.
- Bruckmann, S., Brenn, A., Grube, M., Niedrig, K., Holtfreter, S., von Bohlen und Halbach, O., Groschup, M., Keller, M., & Vogelgesang, S. (2017). Lack of P-glycoprotein Results in Impairment of Removal of Beta-Amyloid and Increased Intraparenchymal Cerebral Amyloid Angiopathy after Active Immunization in a Transgenic Mouse Model of Alzheimer's Disease. *Current Alzheimer research*, 14(6), 656–667. <https://doi.org/10.2174/1567205013666161201201227>
- Burtscher, H. “Physical Characterization of Particulate Emissions from Diesel Engines: a Review.” *Journal of Aerosol Science*, vol. 36, no. 7, 2005, pp. 896–932., doi:10.1016/j.jaerosci.2004.12.001.
- Carson MJ. Microglia as liaisons between the immune and central nervous systems: functional implications for multiple sclerosis. *Glia*. 2002; 40:218–31. <https://doi.org/10.1002/glia.10145>
- Chao CC, Hu S, Ehrlich L, and Peterson PK (1995) Interleukin-1 and tumor necrosis factor- α synergistically mediate neurotoxicity: involvement of nitric oxide and of N-methyl-D-aspartate receptors. *Brain Behav Immun* 9:355–365.
- Chao CC, Hu S, Molitor TW, Shaskan EG, and Peterson PK (1992) Activated microglia mediate neuronal cell injury via a nitric oxide mechanism. *J Immunol* 149:2736–2741
- Cheng, H. et al. Nanoscale particulate matter from urban traffic rapidly induce oxidative stress and inflammation in olfactory epithelium with concomitant effects on the brain. *Environmental Health Perspectives* 124, 1537-1546, doi:10.1289/EHP134 (2016).
- da Fonseca, A. C., Matias, D., Garcia, C., Amaral, R., Geraldo, L. H., Freitas, C., & Lima, F. R. (2014). The impact of microglial activation on blood-brain barrier in brain diseases. *Frontiers in cellular neuroscience*, 8, 362. <https://doi.org/10.3389/fncel.2014.00362>
- Dallas, N.A., Samuel, S., Xia, L., Fan, F., Gray, M. J., Lim, S. J., and Ellis, L. M. Endoglin (CD105): A Marker of Tumor Vasculature and Potential Target for Therapy. *Clinical Cancer Research*, April 2008, 14(7) 1931-1937, doi:10.1158/1078-0432.CCR-07-4478

- Diesel Exhaust and Cancer Risk. (2015). Retrieved from <https://www.cancer.org/cancer/cancer-causes/chemicals/diesel-exhaust-and-cancer.html#:~:text=IARC classifies diesel engine exhaust,diesel exhaust and bladder cancer.>
- Donahue JE, Flaherty SL, Johanson CE, Duncan JA 3rd, Silverberg GD, Miller MC, Tavares R, Yang W, Wu Q, Sabo E, Hovanesian V, Stopa EG. RAGE, LRP-1, and amyloid-beta protein in Alzheimer's disease. *Acta Neuropathol.* 2006 Oct;112(4):405-15. doi: 10.1007/s00401-006-0115-3. Epub 2006 Jul 25. PMID: 16865397.
- Feltrin, C., & Simões, C. M. (2019). Reviewing the mechanisms of natural product-drug interactions involving efflux transporters and metabolic enzymes. *Chemo-Biological Interactions*, 314, 108825. doi:10.1016/j.cbi.2019.108825
- Fonsatti, E., Sigalotti, L., Arslan, P., Altomonte, M., & Maio, M. (2003). Emerging role of endoglin (CD105) as a marker of angiogenesis with clinical potential in human malignancies. *Current cancer drug targets*, 3(6), 427–432. <https://doi.org/10.2174/1568009033481741>
- Fontaine, M., Elmquist, W. F., & Miller, D. W. (1996). Use of rhodamine 123 to examine the functional activity of P-glycoprotein in primary cultured brain microvessel endothelial cell monolayers. *Life sciences*, 59(18), 1521–1531. [https://doi.org/10.1016/0024-3205\(96\)00483-3](https://doi.org/10.1016/0024-3205(96)00483-3)
- Hartz, A. M., Bauer, B., Block, M. L., Hong, J. S., & Miller, D. S. (2008). Diesel exhaust particles induce oxidative stress, proinflammatory signaling, and P-glycoprotein up-regulation at the blood-brain barrier. *FASEB journal: official publication of the Federation of American Societies for Experimental Biology*, 22(8), 2723–2733. <https://doi.org/10.1096/fj.08-106997>
- Haghani, A., Johnson, R., Safi, N., Zhang, H., Thorwald, M., Mousavi, A., Woodward, N. C., Shirmohammadi, F., Coussa, V., Wise, J. P., Jr, Forman, H. J., Sioutas, C., Allayee, H., Morgan, T. E., & Finch, C. E. (2020). Toxicity of urban air pollution particulate matter in developing and adult mouse brain: Comparison of total and filter-eluted nanoparticles. *Environment international*, 136, 105510. <https://doi.org/10.1016/j.envint.2020.105510>
- Jeohn G-H, Kong L-Y, Wilson B, Hudson P, and Hong J-S (1998) Synergistic neurotoxic effects of combined treatments with cytokines in murine primary mixed neuron/glia cultures. *J Neuroimmunol* 85:1–10.
- Jouan E, Le Vée M, Mayati A, Denizot C, Parmentier Y, Fardel O. Evaluation of P-Glycoprotein Inhibitory Potential Using a Rhodamine 123 Accumulation Assay. *Pharmaceutics*. 2016; 8(2):12. <https://doi.org/10.3390/pharmaceutics8020012>

- Juvin, P., Fournier, T., Boland, S., Soler, P., Marano, F., Desmots, J., & Aubier, M. (2002). Diesel Particles Are Taken Up by Alveolar Type II Tumor Cells and Alter Cytokines Secretion. *Archives of Environmental Health: An International Journal*, 57(1), 53-60. doi:10.1080/00039890209602917
- Kauer, J., Schwartz, K., Tandler, C. et al. CD105 (Endoglin) as negative prognostic factor in AML. *Sci Rep* 9, 18337 (2019). <https://doi.org/10.1038/s41598-019-54767-x>
- Kreutzberg, G. W. (1996). Microglia: A sensor for pathological events in the CNS. *Trends in Neurosciences*, 19(8), 312–318. [https://doi.org/10.1016/0166-2236\(96\)10049-7](https://doi.org/10.1016/0166-2236(96)10049-7)
- Kubotera, H., Ikeshima-Kataoka, H., Hatashita, Y. et al. Astrocytic endfeet re-cover blood vessels after removal by laser ablation. *Sci Rep* 9, 1263 (2019). <https://doi.org/10.1038/s41598-018-37419-4>
- Kuhnke D, Jedlitschky G, Grube M, Krohn M, Jucker M, Mosyagin I, et al. MDR1-P-Glycoprotein (ABCB1) Mediates Transport of Alzheimer's amyloid-beta peptides—implications for the mechanisms of Abeta clearance at the blood–brain barrier, *Brain Pathol*, 2007, vol. 17 (pg. 347-53)
- Kwon, HS., Ryu, M.H. & Carlsten, C. Ultrafine particles: unique physicochemical properties relevant to health and disease. *Exp Mol Med* 52, 318–328 (2020). <https://doi.org/10.1038/s12276-020-0405-1>
- Lam FC, Liu R, Lu P, Shapiro AB, Renoir JM, Sharom FJ, et al. beta-Amyloid efflux mediated by p-glycoprotein, *J Neurochem*, 2001, vol. 76 (pg. 1121-8)
- Liu, B., & Hong, J. (2003). Role of Microglia in Inflammation-Mediated Neurodegenerative Diseases: Mechanisms and Strategies for Therapeutic Intervention. *Journal of Pharmacology and Experimental Therapeutics*, 304(1), 1-7. doi:10.1124/jpet.102.035048
- McGuire SO, Ling ZD, Lipton JW, Sortwell CE, Collier TJ, and Carvey PM (2001) Tumor necrosis factor alpha is toxic to embryonic mesencephalic dopamine neurons. *Exp Neurol* 169:219–230
- Michalicova, A., Majerova, P., & Kovac, A. (2020). Tau Protein and Its Role in Blood-Brain Barrier Dysfunction. *Frontiers in Molecular Neuroscience*, 13. doi:10.3389/fnmol.2020.570045
- Löscher, W., Potschka, H. Drug resistance in brain diseases and the role of drug efflux transporters. *Nat Rev Neurosci* 6, 591–602 (2005). <https://doi.org/10.1038/nrn1728>

- Miller, D.S., Bauer, B., Hartz, A.M. Modulation of P-glycoprotein at the blood-brain barrier: opportunities to improve central nervous system pharmacotherapy. *Pharmacological Reviews*, June 2008, 60 (2) 196-209; DOI: <https://doi.org/10.1124/pr.107.07109>
- Mollazadeh, S., Sahebkar, A., Hadizadeh, F., Behravan, J., & Arabzadeh, S. (2018). Structural and functional aspects of P-glycoprotein and its inhibitors. *Life Sciences*, 214, 118-123. doi:10.1016/j.lfs.2018.10.048
- Nel, A. (2005) Atmosphere. Air pollution-related illness: effects of particles. *Science* 308, 804– 806; DOI: 10.1126/science.1108752
- Oberdörster, G., Sharp, Z., Atudorei, V., Elder, A., Gelein, R., Kreyling, W., & Cox, C. (2008). Translocation of Inhaled Ultrafine Particles to the Brain. *Inhalation Toxicology*, 16(6-7), 437-445. doi:10.1080/08958370490439597
- Pan, W., Stone, K. P., Hsuchou, H., Manda, V. K., Zhang, Y., & Kastin, A. J. (2011). Cytokine signaling modulates blood-brain barrier function. *Current pharmaceutical design*, 17(33), 3729–3740. <https://doi.org/10.2174/138161211798220918>
- Pehnek, G., & Jakovljević, I. (2018). Carcinogenic Potency of Airborne Polycyclic Aromatic Hydrocarbons in Relation to the Particle Fraction Size. *International journal of environmental research and public health*, 15(11), 2485. <https://doi.org/10.3390/ijerph15112485>
- Qosa, H., Miller, D. S., Pasinelli, P., & Trotti, D. (2015). Regulation of ABC efflux transporters at the blood-brain barrier in health and neurological disorders. *Brain Research*, 1628(Pt B), 298–316. <https://doi.org/10.1016/j.brainres.2015.07.005>
- Reinhold, A. K. & Rittner, H. L. Barrier function in the peripheral and central nervous system-a review. *Pflugers Arch.* 469, 123–134 (2017).
- Ronaldson, P.T, Bendayan, M., Gingras, D., Piquette-Miller, M., and Bendayan, R. Cellular localization and functional expression of P-glycoprotein in rat astrocyte cultures. *Journal of Neurochemistry*, 22 March 2004, 89 (3) 788-800; DOI: <https://doi.org/10.1111/j.1471-4159.2004.02417.x>
- Rubin, L. L., & Staddon, J. M. (1999). The Cell Biology of the Blood-Brain Barrier. *Annual Review of Neuroscience*, 22(1), 11–28. <https://doi.org/10.1146/annurev.neuro.22.1.11>
- Salter MW, Stevens B. Microglia emerge as central players in brain disease. *Nat Med.* 2017;23:1018–1027.

- Steiner, S., Bisig, C., Petri-Fink, A., & Rothen-Rutishauser, B. (2016). Diesel exhaust: current knowledge of adverse effects and underlying cellular mechanisms. *Archives of toxicology*, 90(7), 1541–1553. <https://doi.org/10.1007/s00204-016-1736-5>
- Süß, P., Lana, A. J., & Schlachetzki, J. (2021). Chronic peripheral inflammation: a possible contributor to neurodegenerative diseases. *Neural regeneration research*, 16(9), 1711–1714. <https://doi.org/10.4103/1673-5374.306060>
- Sydbom, A., Blomberg, A., Parnia, S., Stenfors, N., Sandström, T., & Dahlén, S. (2001). Health effects of diesel exhaust emissions. *European Respiratory Journal*, 17(4), 733–746. doi:10.1183/09031936.01.17407330
- Tai, L. M., Reddy, P. S., Lopez-Ramirez, M. A., Davies, H. A., Male, D. K., Loughlin, A. J., & Romero, I. A. (2009). Polarized P-glycoprotein expression by the immortalised human brain endothelial cell line, hCMEC/D3, restricts apical-to-basolateral permeability to rhodamine 123. *Brain research*, 1292, 14–24. <https://doi.org/10.1016/j.brainres.2009.07.039>
- Tornavaca, O., Chia, M., Dufton, N., Almagro, L. O., Conway, D. E., Randi, A. M., Schwartz, M. A., Matter, K., & Balda, M. S. (2015). ZO-1 controls endothelial adherens junctions, cell-cell tension, angiogenesis, and barrier formation. *The Journal of cell biology*, 2015 March 16, 208(6), 821–838. <https://doi.org/10.1083/jcb.201404140>
- Twigg, By Martyn V., and Paul R. Phillips. “Cleaning the Air We Breathe - Controlling Diesel Particulate Emissions from Passenger Cars.” *Platinum Metals Review*, vol. 53, no. 1, 2009, pp. 27–34., doi:10.1595/147106709x390977.
- Ueda, K., Taguchi, Y., & Morishima, M. (1997). How does P-glycoprotein recognize its substrates? *Seminars in Cancer Biology*, 8(3), 151-159. doi:10.1006/scbi.1997.0066
- Wang, W., Bodles-Brakhop, A. M., & Barger, S. W. (2016). A Role for P-Glycoprotein in Clearance of Alzheimer Amyloid β -Peptide from the Brain. *Current Alzheimer research*, 13(6), 615–620. <https://doi.org/10.2174/1567205013666160314151012>
- Wang, Y., Liu, M., Zhang, J., Liu, Y., Kopp, M., Zheng, W., & Xiao, S. (2018). Multidrug Resistance Protein 1 Deficiency Promotes Doxorubicin-Induced Ovarian Toxicity in Female Mice. *Toxicological sciences : an official journal of the Society of Toxicology*, 163(1), 279–292. <https://doi.org/10.1093/toxsci/kfy038>
- Wang, Y., Xiong, L., Tang, M. (2017). Toxicity of inhaled particulate matter on the

central nervous system: neuroinflammation, neuropsychological effects and neurodegenerative disease. *J. Appl. Toxicol.*, 37 (2017), pp. 644-667.
<https://doi.org/10.1002/jat.3451>

Watson, P. M., Anderson, J. M., Vanlallie, C. M., & Doctrow, S. R. (1991). The tight-junction-specific protein ZO-1 is a component of the human and rat blood-brain barriers. *Neuroscience letters*, 129(1), 6–10. [https://doi.org/10.1016/0304-3940\(91\)90708-2](https://doi.org/10.1016/0304-3940(91)90708-2)

Wei, H., Wei, D., Yi, S., Zhang, F., & Ding, W. (2011). Oxidative stress induced by urban fine particles in cultured EA. hy926 cells. *Human & experimental toxicology*, 30(7), 579-590.

Weksler, B., Romero, I.A. & Couraud, PO. The hCMEC/D3 cell line as a model of the human blood brain barrier. *Fluids Barriers CNS* 10, 16 (2013).
<https://doi.org/10.1186/2045-8118-10-16>

Welser-Alves, J.V., Milner, R. Microglia are the major source of TNF- α and TGF- β 1 in postnatal glial cultures; regulation by cytokines, lipopolysaccharide, and vitronectin. *Neurochemistry International*, 2013 July, 63(1), 47-53.
<https://doi.org/10.1016/j.neuint.2013.04.007>.

“What Is Particulate Matter? | Urban Environmental Program in New England.” EPA, Environmental Protection Agency, March 29, 2022, www3.epa.gov/region1/eco/uep/particulatematter.html .